University of California, Davis
Department of Mechanical and Aerospace Engineering

2026 NASA Human Lander Challenge

Evaporator-Based Potable Water Dispenser for Long-Duration Environmental Control and Life Support Systems

---

Faculty/Staff Advisor:
Dr. Stephen Robinson (stephen.k.robinson@ucdavis.edu)
Professor, Retired NASA Astronaut

Subject Matter Expert:
Janine Moses (janinemoses96@gmail.com)
Thermal Engineer at Intuitive Machines

Undergraduate Students:
Project Co-Lead: Aidan Mateo Guerra (aimguerra@ucdavis.edu)
Project Co-Lead: Andres Mino Cortes (aminocortes@ucdavis.edu)
Project Member: Rachel Lilyanne Long (rllong@ucdavis.edu)
Project Member: Lianne R. de Leon (lrdeleon@ucdavis.edu)

University of California, Davis: Evaporator-Based Potable Water Dispenser (EBPWD)

HuLC HUMAN LANDER CHALLENGE

Theme Subtopic, Major Objectives & Technical Approach:

Theme Subtopic: Potable Water Dispenser

Major Objectives:

- Design, analyze, and test a water dispensing system that has the capability of cooling water with an evaporator.
- Identify and address pain points of previous dispenser iterations.
- Develop a system that prioritizes closed-loop architecture for long-duration missions.

Technical Approach for Each Objective:

- To achieve desired temperatures, water will come in contact with a heating circuit or an evaporation loop with refrigerant R134a.
- Accurate dispense volume will be addressed by mechanically compressing a flexible bladder at a constant rate.
- Redundancy and ergonomics will be incorporated for safety and easy-access maintenance of dispenser, such as a removable filter unit for decontamination.

Image/Graphic:

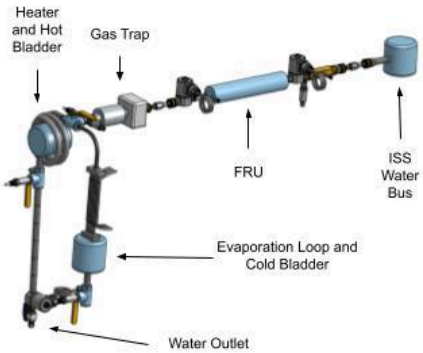

Key Design Details & Innovations of the Concept:

- Design Details and Innovations:
  - First of its kind evaporation cycle with R134a circuit to cool potable water.
  - Hot and cold water flexible bladders to dispense water at accurate volumetric flow rate using mechanical compression.
  - Removable Filter Replacement Unit containing microbial/deiodination filters and UV lights to achieve potable water standards and easy maintenance.
  - Fault detection and incorporation of data panel to monitor key performance parameters such as temperature, pressure, volume, and mass flow rate in real-time.

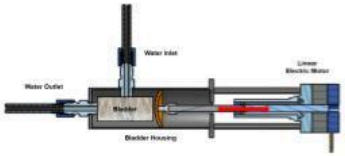

Summary of Schedule & Costs:

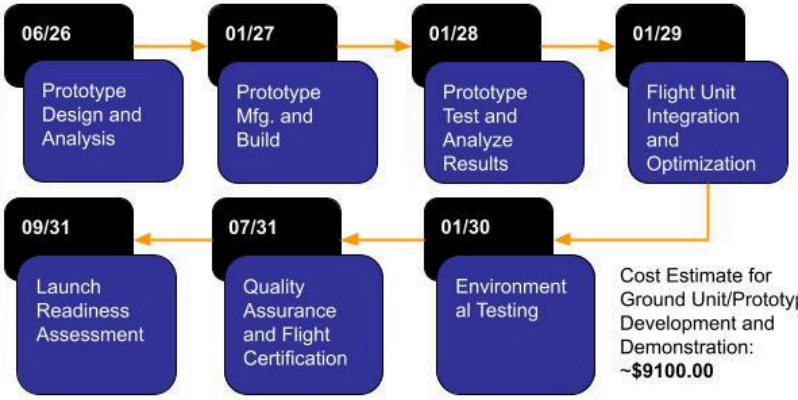

Cost Estimate for Ground Unit/Prototype Development and Demonstration: **~$9100.00**

Contents

1 Executive Summary

With the broadening spaceflight demographic and increasing push of human exploration into Low Earth Orbit (LEO) and beyond, Environmental Control and Life Support Systems (ECLSS) becomes increasingly critical. Increasing mission duration, crew size, and limited resupply challenge the design of ECLSS systems. NASA has identified the need for long-duration ECLSS systems to produce hot and cold water on demand for daily use by astronauts, in order to rehydrate foods and prepare beverages[1]. Current potable water dispensing systems are only capable of producing small amounts of heated water and no cold water. To accomplish this, this proposal highlights the prospects of an evaporator-based potable water dispenser to heat and cool ambient stored water to controlled temperatures for astronaut's food and beverage needs. Thermal management devices, fluid components, and decontamination filters are incorporated into the proposed design to meet NASA's requirements for temperature controlled water, potable water standards, and sustained lunar presence.

2 Introduction

2.1 Problem Statement and Background

The Potable Water Dispenser (PWD) was first developed as early as the 1960s–1970s for the Gemini and Apollo Programs as a means to provide safe drinking water for in-space applications in efforts to advance NASA ECLSS for human sustainability[2]. As human space missions expanded in duration and complexity, reliable water delivery systems became essential for crew health, hydration, and food preparation.

Figure 1: First PWD Flight Unit[21].

Since its development, the PWD has gone through several iterations and has been found in multiple spacecraft (e.g., Space Shuttle missions) and is currently used aboard the International Space Station (ISS) as the primary means of drinking water and food/beverage rehydration methods[3]. However, as missions expand beyond Low Earth Orbit (LEO), the importance of reliability and capability becomes increasingly critical, especially for life support in Gateway, as highlighted in NASA's Plan for Sustained Lunar Exploration and Development[4]. Current PWD systems, although functional, are limited in their ability to dispense highly accurate volumes of potable water and to provide water temperatures below ambient (20–25°C). Furthermore,

existing PWD designs have experienced issues such as corrosion in the dispensing needle, material degradation within internal flow paths, microbial accumulation in wetted components, valve leakage, and seal wear over extended operational periods[5]. Despite these efforts, there are currently no on-orbit solutions that provide both hot, cold, and ambient water for astronauts simultaneously.

Figure 2: Leidos Exploration Potable Water Dispenser (xPWD)[22].

Moreover, although evaporators have been used on the ISS and spacesuits historically, they are not widely known or researched for uses such as potable water dispensing[6].

2.2 Proposed Solution

As a result, the aim of the EBPWD is to improve upon existing designs of potable water dispensers, such as the one on the ISS, by enabling water cooling below ambient temperature ranges through the use of an evaporation cycle. Moreover, the project also aims to address the shortcomings of previous dispenser iterations, such as inaccurate dispense volume and system pressure loss[5]. These goals will be achieved with three methodological design objectives, which drive the system and subsystem requirements.

Objective 1: *Design, analyze, and test a water dispensing system that has the capability of cooling water with an evaporator.* To achieve desired temperatures, water will come in contact with an electrical heating circuit or an evaporation loop with refrigerant R134a.

Objective 2: *Identify and address pain points of previous dispenser iterations.* Accurate dispense volume will be addressed by mechanically compressing a flexible bladder at a constant rate.

Objective 3: *Develop a system that prioritizes closed-loop architecture for long-duration missions.* Redundancy and ergonomics will be incorporated for safety and easy-access maintenance of dispenser, such as a removable filter unit for decontamination.

2.3 Changes From Proposal

Since the proposal, Objective 2 was modified to descope the redesign of the dispense needle, as issues with corrosion and backflow were already previously addressed[23]. Additionally, the scope of Objective 3 was adjusted to prioritize formulation of a closed-loop architecture for long-duration operation. Additionally, the overall system architecture (see Section 3.2) was

updated incorporating feedback from the initial proposal regarding gas trap location and ambient water flow path.

3 Technology Approach and Concept

3.1 System Requirements

Table 2 outlines the top level system requirements for the EBPWD, which are derived from the overarching needs of NASA's Artemis Program. These requirements translate the project objectives into measurable, and verifiable needs that will guide all subsequent design, development, and project management. Each requirement was formulated based on functional expectations and customer constraints from the NASA HuLC, along with design considerations from NASA technical specification documents[7,8]. Verification of these requirements will be accomplished through one of four methods. Inspection will be conducted through visual examination of drawings and CAD assembly/part models. Analysis will be achieved through hand-calculations and computer simulations (heat transfer, fluids, etc.). Demonstration and testing will be performed by modeling system and subsystem performance under simulated environmental conditions. Many of these requirements cannot be fully verified without physical testing of prototypes to test their feasibility, as many components have not been used for this particular application.

The EBPWD consists of the following subsystems: Thermal (TH), Electrical (EE), Structural (SC), and Decontamination (DC). The tables, listed in the Appendix, outline the subsystem level requirements for the EBPWD. These requirements will translate each subsystem objective into measurable and verifiable needs that will meet the top level system requirements.

3.2 System Overview and Architecture

The system and subsystem requirements above were used to develop a preliminary design for the EBPWD, which is currently at TRL 2. Further hand calculations and computer simulations will be conducted to further mature the validity of the design prior to manufacturing, procurement, and testing.

The Piping and Instrumentation Diagram (P&ID) in Figure 3 displays how astronauts will obtain potable water from the water supply (22.5 psig and 22.5 °C). The entire dispenser is powered through a 28 Vdc auxiliary output, which will connect to ISS EXPRESS Rack 6[13]. The ISS EXPRESS Rack 6 can provide up to 2000 Watts of power (28 Vdc), and at most 20 amps[13]. A temperature transducer will be installed after the water supply to gauge the temperature, compare it to the input temperature, and actuate the temperature selection valve to decide where the filtered water will go via electrical actuation. The design also features a Filter Replacement Unit (FRU), which consists of a deiodination filter, microbial filter, and ultraviolet (UV) light. Check valves are incorporated to ensure one way transport of the water throughout the unit. A pressure transducer and temperature transducer are incorporated after the FRU to determine if the water needs to be heated or cooled, through a temperature selection valve. The heater and evaporator will heat/cool the water stream. The evaporation system consists of an evaporator, which feeds to a separate R134a refrigerant loop featuring a peristaltic pump, phase separator, condenser, and expansion valve. A peristaltic pump was selected to push the

refrigerant due to its low maintenance (no moving parts) and zero contamination/leakage. R134a was selected as the evaporator working fluid as it is low cost, non-toxic, non-flammable, and has the previous heritage of being used for water chillers and automobile air conditioning on Earth[15]. Although ammonia is used on the ISS, it was not selected for this application as it is toxic and flammable, which increases the risk of operation.

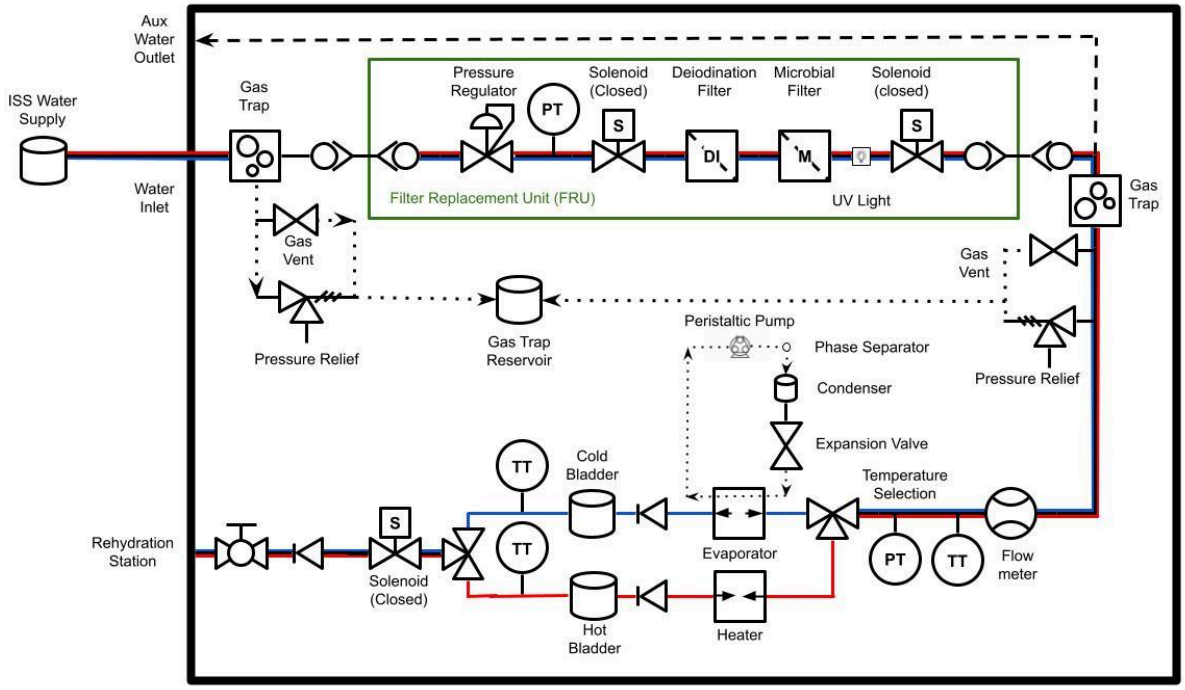

Figure 3: EBPWD P&ID. See Appendix for P&ID Key.

As the water is heated/cooled, it feeds into a flexible bladder, which is then dispensed at a volumetric flow rate of 500 mL/min through a needle at the exit interface using mechanical compression to squeeze the water out. The design features Quick Disconnects (QDs) for easy access maintenance in the event of a leak or filter replacement. When the FRU is maintenanced, air may become trapped in the QDs, therefore a gas trap and gas vent were incorporated before and after the FRU. Both gas vent and pressure relief valves release into a gas trap reservoir/bladder.

If the water quality levels exceed 50 CFU/mL, then the FRU needs to be flushed. See the ConOps section which discusses how often the crew should check the water quality levels. For the flush case, the EBPWD will feature a storage compartment unit containing two Teflon bags of 40 ppm I_2 solution and a microbial check device[14]. The FRU can be disconnected from the EBPWD by closing the solenoid valves, where it will interface with one of the Teflon bags. Sterile caps will be used to plug the quick disconnects in the dispenser to prevent contamination. After flushing with iodine, the FRU will then be flushed with 10 L of water. The water quality will be measured using the microbial check device before and after the iodine flush, at the outlet of the FRU.

For redundancy, within the dispenser's housing storage compartment exists a backup microbial and deiodination filter in the event that the pre-installed filters fail within 12 months of first dispense. Moreover, the storage compartment will contain the necessary tools for maintenance in the event of a leak or other system fault. Future design iterations may include additional features such as ISRU compatibility, for example, water ice processing or filtering water from lunar ice deposits.

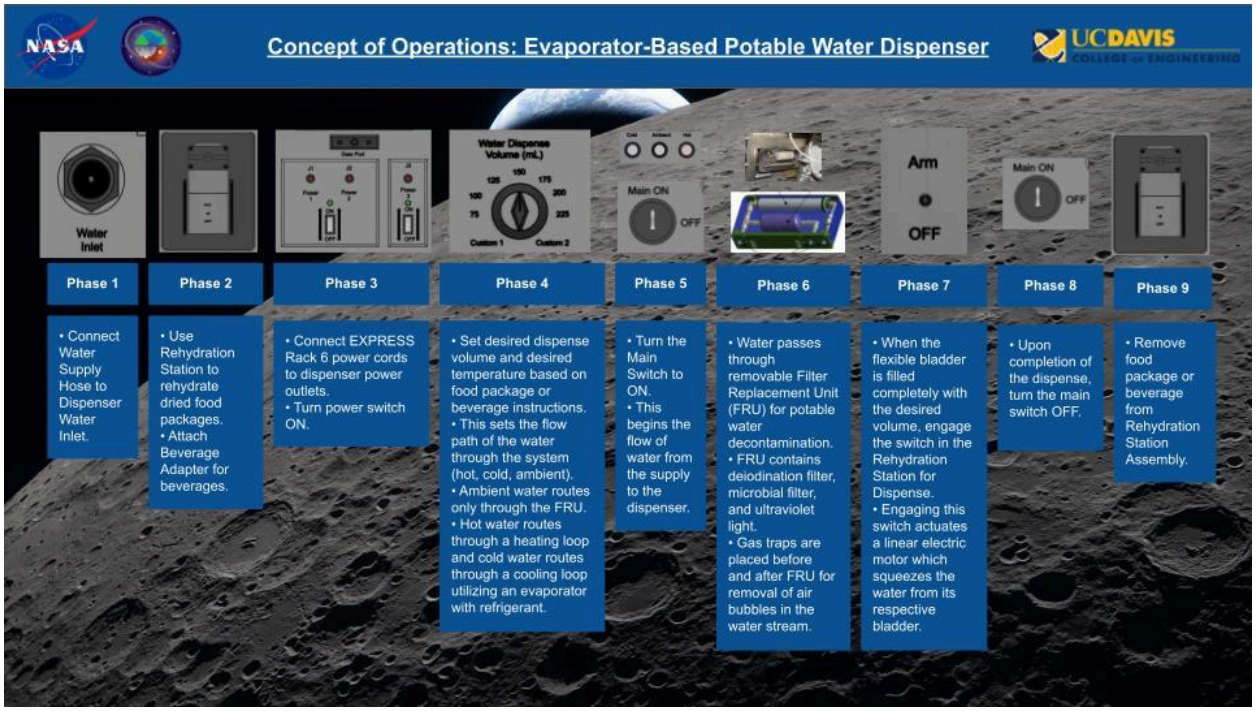

Figure 4: EBPWD Concept of Operations (ConOps).

The ConOps above shows how the EBPWD will be demonstrated to achieve the methodological objectives and meet the system requirements throughout the mission lifecycle.

3.3 Assumptions

Assumptions were made in order to make this project realistic and flexible for future adaptation. First, the design assumes that similar ISS EXPRESS rack technology for payloads/experiments will be used on Lunar/Martian bases and space stations. Second, the rack structure is assumed to be flight-qualified. For the heating and cooling calculations, the following assumptions were made: constant water properties, constant material properties, uniform coil temperature, perfect bladder mixing, one-dimensional radial heat transfer, negligible radiation heat transfer, and constant heater efficiency.

4 Conceptual Engineering Design and Analysis

4.1 Heating and Cooling Design

The EBPWD thermal design is divided into two primary subsystems: the heating subsystem and the cooling subsystem. Together, these subsystems allow the dispenser to provide temperature-controlled potable water. The heating subsystem raises incoming, compressed potable water to the required hot-water temperature range, while the cooling

subsystem lowers incoming potable water below ambient temperature using an evaporator-based cooling loop.

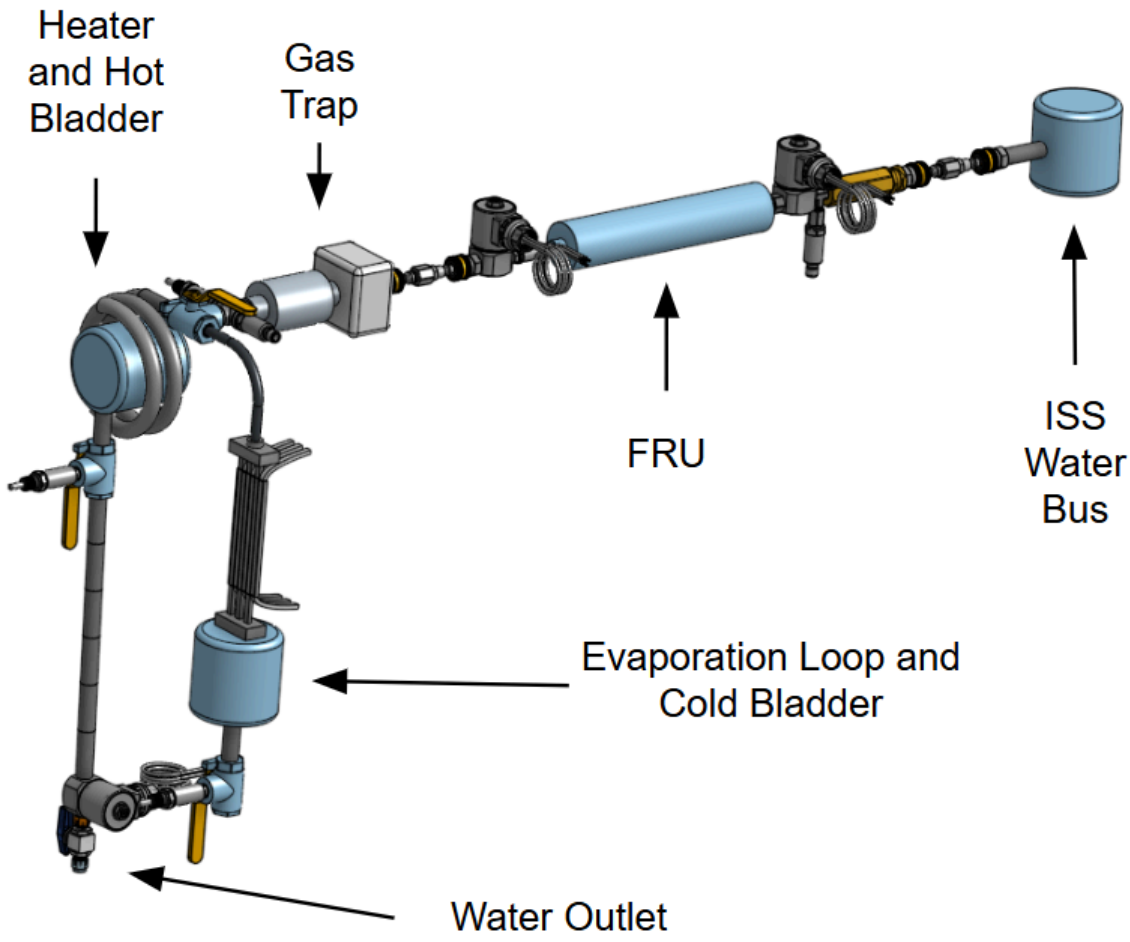

Figure 5. Open test stand CAD model of the heating and cooling subsystems interfaced with the feed system. The open lines on the evaporation loop represent the cooling microchannels that will run to the unmodeled peristaltic pump and condenser.

The current configuration supports early testing and integration, and will later be condensed into the dispenser housing after component sizing and validation. The thermal design is evaluated using a spreadsheet calculator that models transient heat transfer, fluid accumulation, and dispensed water temperature over time (See Appendix). The calculator supports early sizing of the heater, cooling channel length, flow rate, compressible bladder volume, and insulation requirements. It also provides a first-order method for checking whether the system can satisfy the thermal subsystem requirements prior to higher-fidelity simulation and prototype testing.

The main purpose of the heating and cooling calculator is to estimate the temperature of water at the point of dispense. For both subsystems, the most important output is not only the instantaneous outlet temperature, but also the average temperature of the water collected in the bladder before release. This is important because the water that is ultimately dispensed is

collected over time, so the final usable temperature depends on the transient temperature history of the water entering the bladder. The calculator uses thermal resistance methods, transient energy balances, and explicit time stepping. Thermal resistances are used to estimate heat transfer through convection, conduction, insulation, and ambient losses. Energy balances are used to update the water temperature in the heating or cooling section. Explicit time stepping is then used to calculate how the temperatures, heat transfer rates, and bladder volume change with time. A detailed equation breakdown is provided in the Appendix.

The thermal subsystem analysis is currently preliminary and is intended for conceptual engineering design. The results will be used to guide component sizing, identify critical design sensitivities, and support the selection of heater power, tube length, cooling channel length, flow rate, and insulation thickness. The model will later be refined through higher-fidelity thermal-fluid simulation and experimental testing.

4.1.1 Heating Subsystem

The heating subsystem is designed to raise ambient potable water to the required hot-water temperature range for food and beverage rehydration. In the current concept, water from the main supply is routed through a heated tube or coil that is thermally coupled to an electric heater. Heat transfers from the heater surface through the tube wall and into the flowing water before the heated water collects in the hot bladder.

The heating calculator models the heated tube as a transient control volume. It tracks the temperature of the water inside the heated section and the average temperature of water collected in the hot bladder. The model also accounts for heat transfer into the water and heat loss to the surrounding environment through the insulated heater assembly. The main heating inputs include the incoming water temperature, target hot-water temperature, target bladder volume, heater power, heater efficiency, tube dimensions, insulation properties, water properties, flow rate, and timestep. The most important sizing variables are heater power, heated tube length, flow rate, and insulation thickness. Increasing tube length improves heat transfer area and residence time, but also increases mass, packaging volume, and pressure drop.

To size the heating subsystem, the calculator is used to vary the heated tube length while holding the main design assumptions constant. The preferred length is the shortest length that allows the collected bladder water to reach the required hot-water temperature range with reasonable margin. This approach avoids unnecessary heater length while still satisfying the thermal requirement.

The heating model is intended as a preliminary sizing tool. It assumes constant water and material properties, a lumped water temperature in the heated section, negligible radiation heat transfer, and well-mixed bladder contents. These assumptions will be refined through higher-fidelity thermal-fluid simulation and prototype testing.

4.1.2 Cooling Subsystem

The cooling subsystem is designed to cool potable water below ambient temperature before dispense. In the current concept, room-temperature source water is pushed through selected square microchannels in a multichannel heat exchanger, while a peristaltic pump circulates refrigerant through every other square microchannel. This alternating water–refrigerant channel arrangement increases the shared wall area available for heat

transfer. Heat is transferred from the water, through the shared channel walls, and into the closed-loop refrigerant before the cooled water collects in an insulated cold bladder for dispense. The cold bladder is modeled as initially empty. This means the bladder is filled only by water that has already passed through the cooling channels. Therefore, the bladder temperature is calculated as the running average of the cooled outlet water entering the bladder, rather than as a reservoir of room-temperature water being cooled in place.

The cooling calculator estimates outlet water temperature, average cold bladder temperature, heat removed from the water, heat rejected to the refrigerant, ambient heat leak, and bladder fill volume over time. The detailed equation breakdown is provided in the Appendix. In the current setup, the volumetric flow rate is 500 mL/min, so the bladder fill volume increases with time until the target volume is reached. The main sizing variables are cooling channel length, number of water channels, refrigerant-side boundary temperature, flow rate, and insulation effectiveness. The optimal cooling length is the shortest channel length that allows the average cold bladder temperature to meet the target by the time the bladder reaches the desired dispense volume.

4.2 Structural and Mechanical Design

The structural and mechanical design of the EBPWD encompasses the dispenser housing, interface panel, and compressible bladder assembly. CAD models were developed to size these components based on provided ISS EXPRESS rack dimensions and dispense volume requirements.

4.2.1 Dispenser Housing

The dispenser housing was designed to fit within two stacked ISS Shuttle Middeck lockers, similar to the PWD and xPWD[24]. The interface panel features two large handrails on the side to allow users to perform maintenance on key components such as fittings and valves. This interface panel can be removed from the main housing by rotating the knobs on each of the four corners. The panel rests on a rail-system that allows the contents on the dispenser to slide out for easy access. The internal volume houses about 4.06 cubic feet, with the entire housing structure being 23.00 inches in height, 18.50 inches in width and 21.50 inches in depth.

Figure 6: CAD Model of the EBPWD Housing with Interface Panel.

4.2.2 Interface Panel

The design for the interface panel was inspired by the designs of the existing PWD and xPWD, combining the advantages of both designs. The interface panel incorporates inlet and outlet fans to promote convective heat transfer, managing thermal loads generated by the cooling loop condenser and the electronics mounted on the backside of the panel. For diagnostics and commanding, a Fault LED identifies off-nominal behavior, while a Ground Control LED indicates when ground operators have taken control of the dispenser during an anomaly. Active system monitoring, which is crucial for long-duration missions, is facilitated by an integrated data port; this port feeds telemetry to the rear electronics board, allowing the onboard computer to detect faults and illuminate the diagnostic LED. Power interface is established via J1, J2, and J3 outlets that plug directly into the EXPRESS Rack. Users can select cool, hot, or ambient water via three dedicated control buttons, while water routing is managed through a primary inlet water port and an auxiliary water port used to fill contingency water containers (CWCs), which routes water exclusively through the FRU. The bottom right of the panel features the removable FRU rack, which can slide out by pulling the handrails.

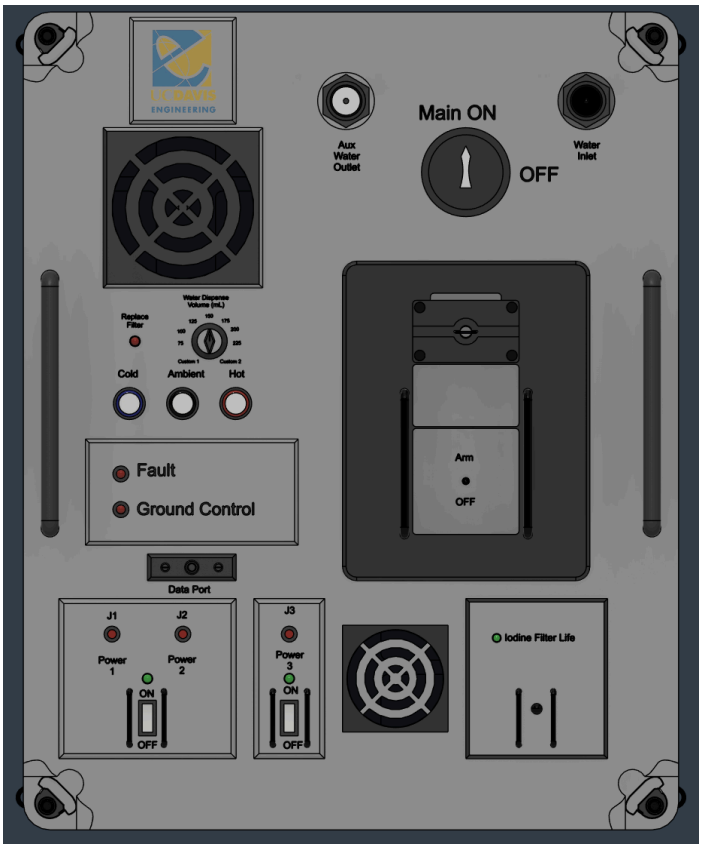

Figure 7: CAD Model of Interface Panel.

4.2.3 Compressible Bladder Assembly

As traditional cylindrical and spherical tanks fail to manage fluids in microgravity, an alternative storage method for the heated and cooled water was required. Drawing inspiration from Washington State University's Hydrogen Properties for Energy Research (HYPER) Laboratory, a flexible bladder assembly was developed[25].

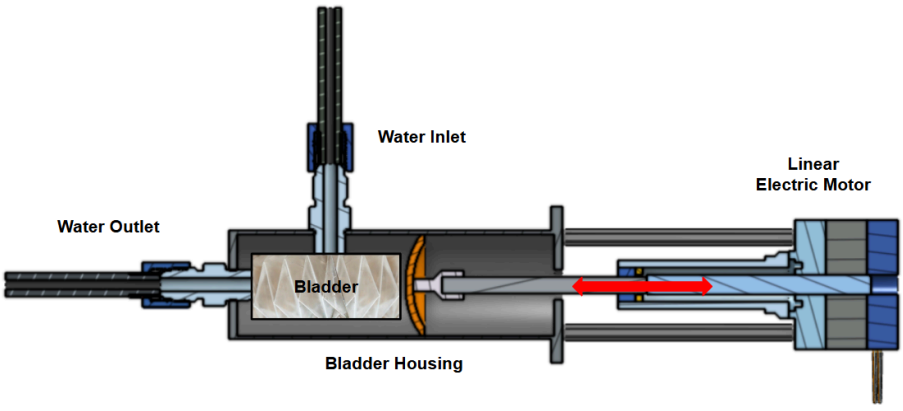

Figure 8: CAD Model of Flexible Bladder Assembly.

This system utilizes a linear electric motor to compress the flexible bladder, dispensing the stored water from the water outlet once the bladder reaches the desired volume.

4.3 Decontamination

The decontamination architecture consists of two filters arranged in series within the EBPWD Filter Replacement Unit (FRU): an Activated Carbon/Iodine Exchange (ACTEX) filter and a 0.2-micron microbial filter[30,32,16]. Incoming water from the ISS Water Bus contains residual iodine, which is intentionally used as a biocide to prevent biofilm formation and bacterial colonization within the internal plumbing of the EBPWD[28]. The water is typically maintained within a concentration range of 1–4 ppm of I_2; however, this exceeds the maximum allowable concentration for potable water as defined by NASA health standards (0.2 ppm)[26,30,32].

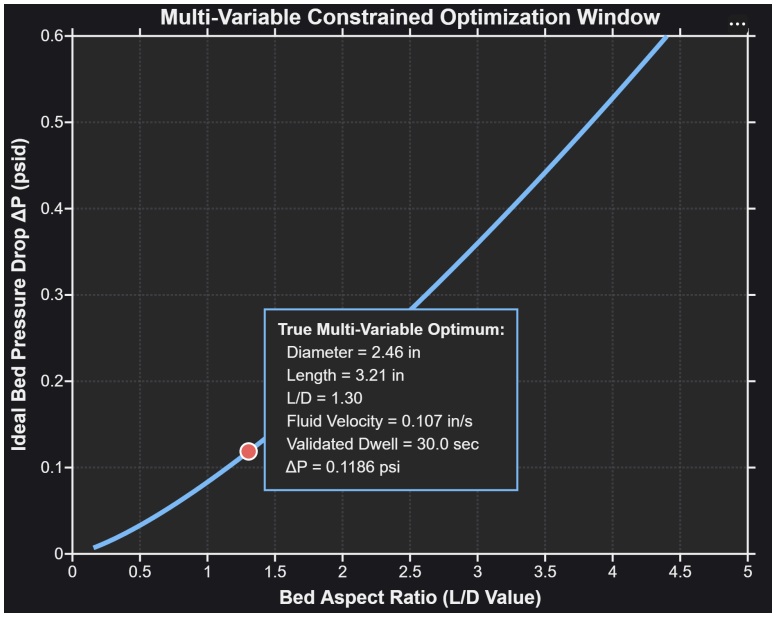

Figure 9: Resin Bed Sizing, optimized L/D ratio, used legacy ACTEX as reference[27]

To address this requirement, the ACTEX unit reduces iodine concentration through adsorption and ion exchange processes, utilizing granular activated carbon to adsorb molecular iodine (I_2) and a strong-base anion exchange resin to remove iodide ions (I^-)[27,30,16]. Additionally, within the ACTEX cartridge are internal particulate filtration elements—specifically, structural mesh screens responsible for retaining the media beds, trapping shedding chemical fines from the carbon and resin matrices, and protecting downstream plumbing and the separate microbial filtration stage from fouling and particulate accumulation[27]. The chemical resin bed possesses a volume of 250 cc with an operational life of approximately 7-months, while the integrated particulate filters maintain a projected operational life of 12-months[27]. However, because the ACTEX cartridge is serviced as a single, replaceable unit, the entire assembly must be replaced within a 7-month interval despite the 12-month operational life of the particulate filters.

The separate microbial filtration stage provides the final microscopic particulate and biological reduction prior to dispensing[27]. This stage utilizes a 0.2-micron hydrophilic Nylon 6,6 membrane supported structurally by a rigid polypropylene housing[30]. Although the ISS Water Bus is treated with iodine to prevent biofilm formation and bacterial colonization, microbial organisms and other pathogenic contaminants may still persist even in the presence of biocidal agents[30,32]. The exact microbial loading conditions of the ISS water supply are not explicitly

defined in available literature in terms of colony-forming units per milliliter (CFU/mL); however, potable water standards require that microbial concentrations remain below the maximum allowable limit of 50 CFU/mL[26,30,32]. Subsystem performance was modeled using an operational Log Reduction Value (LRV) target of 3.0 for the microbial filtration stage, representing a worst-case microbial loading scenario, to ensure compliance with water quality standards[20,30,32].

Design considerations addressed within the EBPWD are intended to satisfy the requirements imposed by the International Conference on Environmental Systems (ICES), while also mitigating previous issues known to hinder PWD performance, most notably pressure losses throughout the decontamination subsystem and associated flow architecture[27]. The EBPWD, like its counterparts, will remain modular to allow for easy access and replacement of filters within the FRU[32].

Furthermore, the ideal volume of the resin bed was calculated based on the total expected mass of influent iodine (I_2) and iodide (I^-) over the projected operational lifetime of the subsystem (7 months)[16]. The sizing matrix required a chemical removal efficiency sufficient to reduce incoming biocide concentrations ranging from 1–4 ppm to below the required threshold of 0.2 ppm. To achieve this efficiency, the dwell time of the incoming water within the packed bed was calculated to be a minimum of 30 seconds, ensuring sufficient chemical contact time for coupled adsorption and ion-exchange kinetics to effectively remove iodine from the water supply[27]. However, increasing resin bed length also increases pressure losses throughout the subsystem[16,27]. To mitigate these effects, the EBPWD evaluated and refined the resin bed geometry (specifically adjusting the length-to-diameter, or L/D ratio) to minimize pressure losses while still satisfying the required contact time constraints imposed by the pressure-driven pumping architecture[27]. An optimal resin bed geometry was therefore determined that achieved the required decontamination efficiency without inducing excessive system strain or reducing flow performance[27]. See Appendix for filter sizing equations, MATLAB code, and additional references.

4.4 Controls and Electrical

A flow control diagram (Figure 10) was developed to outline the architecture of the main control computer, which processes environmental telemetry and user inputs to manage the EBPWD. These electronics will be mounted on the backside of the interface panel. This flow control diagram was inspired by the flow control electronics developed by NASA engineers during a troubleshooting investigation in mid-July 2009 when the original PWD began experiencing inaccurate dispense volumes[33]. For long-duration missions, active monitoring of systems such as the potable water dispensing become crucial.

On the input side, physical data from pressure, temperature, and mass flow sensors are digitized via an Analog-to-Digital Converter (ADC) and fed into the Volume Control Module, while physical control switches route the user commands to the Input Controls Logic. Inside the main controller, these two modules work interchangeably with the Valves Control Module and Filter Tracking Logic to continuously calculate dispense volumes, monitor filter lifespans, and determine when to actuate fluid hardware.

On the output side, the Valves Control Module drives the physical hardware by signaling Valve Drivers to actuate the system's solenoid valves, while commanding the LED control module to update status and fault indicators on the interface panel.

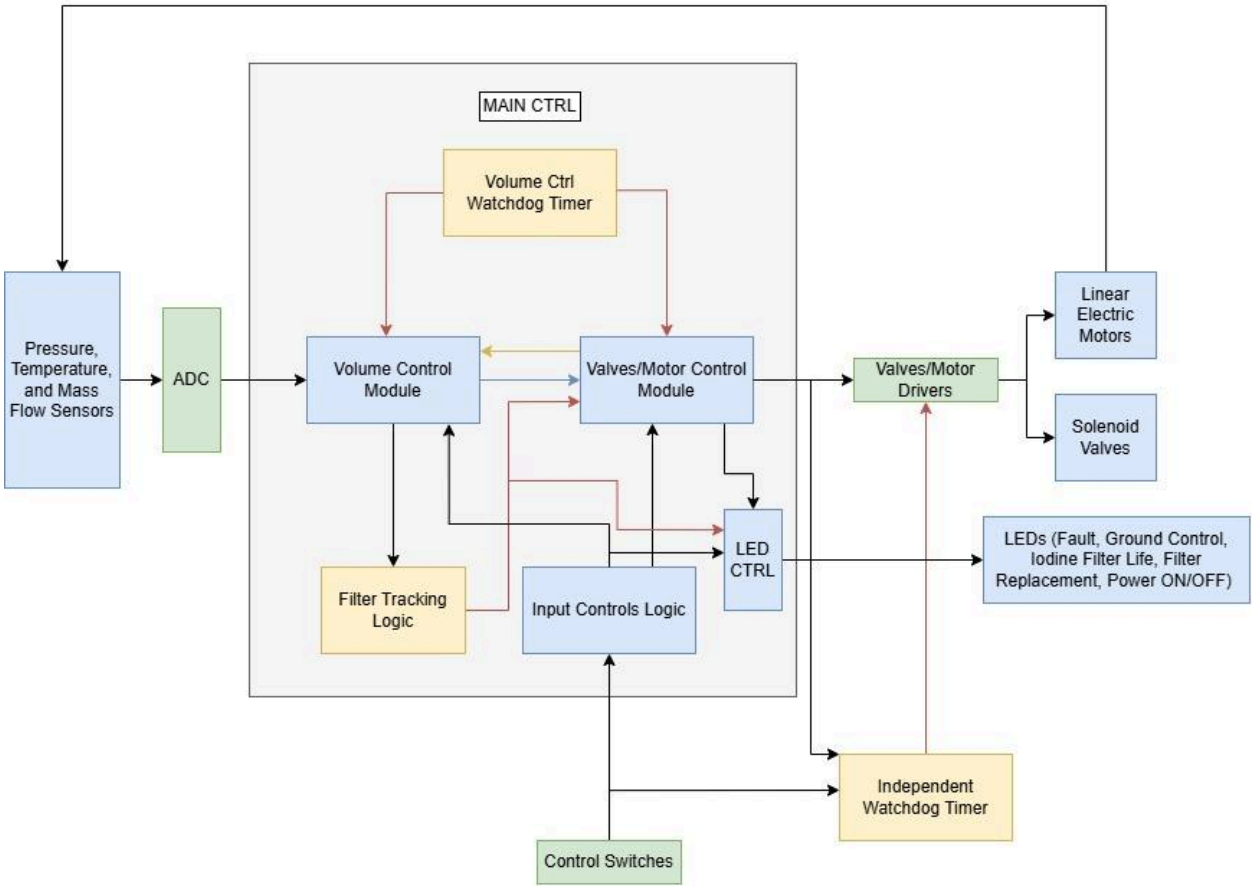

Figure 10: EBPWD Flow Control Electronics Diagram.

System safety and redundancy are enforced by the internal volume control watchdog timer that monitors the main control modulus and an external independent watchdog timer. This independent timer tracks both user switch inputs and raw valve inputs, which allows it to override the drivers and shut down the system if an operational anomaly occurs. A feedback loop is incorporated from the linear electric motor to the ADC and pressure sensors to monitor the accuracy of the dispense volume.

5 Technical Management

5.1 Risk Assessment and Mitigation

To analyze and mitigate any risks posed by the EBPWD, a 5x5 risk matrix (Figure 11) was developed to track risk across the system's development. The matrix compiles 5 relevant critical risks to determine likelihood and consequences. These risks are (1) biofilm development under stagnant conditions, (2) inaccurate dispense volume, (3) inaccurate outlet temperature, (4) inaccurate dispense flow rate, and (5) unknown science behind fluid behavior in microgravity. This matrix was built following the guidelines provided in the NASA Risk Management Handbook (NASA/SP-2011-3422)[12]. Risk posture (likelihood and consequence) will be refined and reduced through further research, design, and simulation.

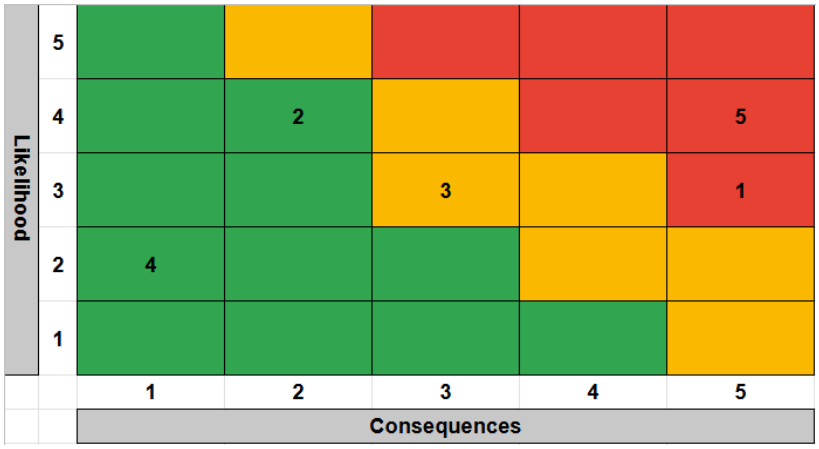

Figure 11: EBPWD Risk Matrix

5.2 Project Timeline and Budget Estimate

The following section describes scheduling, manufacturing, and testing plans for the EBPWD project. The timeline for the EBPWD spans 5 years from January 2026 (TRL 1) to December 2031 (TRL 7), detailing the structured phases essential to project success. Team/Faculty Meetings will occur monthly, along with monthly documentation, design reviews, and reporting. The Design Phase spans from January 2026 to December 2026 (raise to TRL 3), with the Manufacturing Phase beginning January 2027 (raise to TRL 4). A full breakdown of the project lifecycle and timeline can be seen in the Gantt Chart, which is listed in the Appendix.

Product Lifecycle Management will be used to manage the project's journey from design to manufacturing. Custom parts and COTS parts will all be assigned their own part numbers for record keeping as the project matures. Furthermore, a Bill of Materials will be developed including information on part number, descriptions, quantities, unit costs, and suppliers when the dispenser design is finalized. To facilitate the production process, prototypes will be manufactured and tested at the UC Davis ESDC and TEAM Lab.

To verify system and subsystem requirements, four performance metrics will be evaluated: temperature accuracy, volumetric accuracy, microbial count, and flow rate accuracy. Individual component tests will also be performed to characterize parameters such as pressure drop across components. These tests will be conducted using thermocouples and flow meters, and precision scales – for each component and the entire system fully integrated. Comprehensive testing plans will be developed by Fall 2026 to ensure that the dispenser test stand and procedures are compliant with the UC Davis ESDC safety protocols.

Environmental verification will follow the guidelines of the NASA General Environmental Verification Standard (GEVS), GSFC-STD-7000B, and will be traceable to system and subsystem requirements through a verification matrix[10]. As the EBPWD will operate only within the pressurized cabin of a space station or space habitat, qualification will focus on internal vehicle environments as opposed to the external deep-space environment. Thermal testing will be conducted in a controlled-air environment to validate performance within cabin temperature limits. Launch survivability will be verified through hand calculations, finite element analysis (FEA), random vibration, shock, and structural loading tests consistent with current launch vehicle environments. Radiation tolerance will be assessed through analysis and

component-level testing appropriate for total ionizing dose levels for lunar/Martian transit and surface environments.. Electromagnetic compatibility testing will also be performed to ensure dispenser electronics are compliant with cabin electromagnetic interference requirements. Upon completion of integrating the flight-unit, facilities will be identified to support thermal, structural, radiation, and EMC verification. Moreover, all materials will be tested for flammability and arc tracking for wires, following the guidelines of NASA-STD-6001[11].

Currently, the EBPWD project has received funding from Phase 2 of the 2026 NASA Human Lander Challenge and the California Space Grant Consortium through the 2026 CaSGC Student STEM Collaborative Project Award. The total funds ($11,500) from both sources will be used to build prototypes and the dispenser ground unit whose results will inform the development of a flight-ready unit. Table 1 (See Appendix) shows the Ground Unit Budget Table for cost estimates. Upon completion of the Bill of Materials for the final dispenser design, the development and operating costs of the flight unit will be projected using the NASA Project Cost Estimating Capability (PCEC)[34].

5.3 Conclusion and Future Work

The team has spent the last 5 months developing the design of the EBPWD through extensive research, trade studies, and calculations, resulting in a preliminary design that features the dispenser housing, a compressible bladder assembly to provide an accurate water flow rate, and heating/cooling architecture to alter the temperature of the supply water. Prototype development and testing will demonstrate the prospect of the EBPWD for long-duration applications to lunar and Martian missions. Further design work, simulations, and research will be conducted, especially to further understand the behavior of fluids in microgravity. This work will constrain the final design of the EBPWD. Beyond the 2026 NASA HuLC Forum, the team aims to continue development of the EBPWD through the use of the CaSGC and HuLC Phase 2 funds. Next steps will include the following:

- Housing and FRU rail system CAD modeling
- Sizing and design of filters and UV Light in the FRU
- Extend longevity of filters for longer duration missions
- Research anti-fouling/omniphobic surface coatings for filter screens to prevent particulate and microbial adhesion, minimizing pressure losses
- High-fidelity simulations for heating and cooling loops in Thermal Desktop
- Develop simulations and hand calculations for flexible bladder compression
- Storage compartment design
- Compacting fluid circuit into internal dispenser housing volume
- Electronic circuit and PCB design for fluid flow control
- Launch load and vibrational analysis of housing structure in Patran/Nastran
- Power draw calculations from electronics, heater, valves, and other fluid components

The EBPWD team would like to extend its appreciation towards the National Institute of Aerospace (NIA), NASA, and the California Space Grant Consortium for the opportunity to technically develop a unique ECLSS research concept. The team would also like to recognize the invaluable oversight of faculty advisor Dr. Stephen Robinson and subject matter expert Janine Moses. Finally, the EBPWD team thanks the University of California, Davis, for its dedication to space research, education, and support of student engineering design teams.

Appendix

References

[1] Ebarle, G. (2026). *2026 Human Lander Challenge (HuLC) Guidelines*. https://hulc.nianet.org/wp-content/uploads/2026-Human-Lander-Challenge-HuLC-Proposal-Guidelines.pdf

[2] *Water Dispenser, Gemini, Training | National Air and Space Museum*. (n.d.). Retrieved March 2, 2026, from https://airandspace.si.edu/collection-objects/water-dispenser-gemini-training/nasm_A19680274000

[3] *ISS Daily Summary Report – 8/31/2023—NASA*. (2023, August 31). https://www.nasa.gov/blogs/stationreport/2023/08/31/iss-daily-summary-report-8-31-2023/

[4] United States National Aeronautics and Space Administration. (2021). *NASA's plan for sustained lunar exploration and development.* National Aeronautics and Space Administration. https://www.nasa.gov/wp-content/uploads/2020/08/a_sustained_lunar_presence_nspc_report4220final.pdf?emrc=5aa8ef

[5] Shaw, L. A., & Barreda, J. L. (2008, January 1). *International Space Station USOS Potable Water Dispenser Development*. 38th International Conference on Environmental Systems. https://ntrs.nasa.gov/citations/20080013432

[6] Bue, G. C., Makinen, J. V., Miller, S., Campbell, C., Lynch, B., Vogel, M., Craft, J., & Petty, B. (2014, August 4). *Spacesuit Water Membrane Evaporator; An Enhanced Evaporative Cooling Systems for the Advanced Extravehicular Mobility Unit Portable Life Support System*. https://ntrs.nasa.gov/citations/20140010666

[7] *6.0 Natural and Induced Environments—NASA*. (n.d.). Retrieved March 2, 2026, from https://www.nasa.gov/reference/6-0-natural-and-induced-environments-vol-2/

[8] Leahy, F. B. (2021, October 27). *SLS-SPEC-159, Cross-Program Design Specification for Natural Environments (DSNE)*. https://ntrs.nasa.gov/citations/20210024522

[9] Moran, M. J., Shapiro, H. N., Boettner, D. D., & Bailey, M. B. (2014). Fundamentals of engineering thermodynamics. John Wiley & Sons.

[10] *General Environmental Verification Standard (GEVS) for GSFC Flight Programs and Projects | Standards*. (n.d.). Retrieved March 2, 2026, from https://standards.nasa.gov/standard/GSFC/GSFC-STD-7000

[11] *Flammability, Offgassing, and Compatibility Requirements and Test Procedures | Standards*. (n.d.). Retrieved March 2, 2026, from https://standards.nasa.gov/standard/NASA/NASA-STD-6001

[12] Dezfuli, H., Guarro, S., Everett, C., Benjamin, A., & Skow, M. C. (2024, November 1). *NASA Risk Management Handbook: Version 2.0, Part 1*. https://ntrs.nasa.gov/citations/20240014019

[13] Davis, T. B., Adams, J. B., Fisher, E. M., Prickett, G. B., & Smith, T. G. (1999). *EXPRESS Rack Technology for Space Station*. https://ntrs.nasa.gov/citations/19990008536

[14] *[Environmental Health] NLSP*. (n.d.). Retrieved March 2, 2026, from https://nlsp.nasa.gov/explore/jtable/lsda_document/lsda_document?q=all&from=1&pagesize=100&filters=research_name.keyword%7Cmm%7CEnvironmental%20monitoring,Microbiology;project_name.keyword%7Ceq%7CMRID&template=5

[15] McCullough, E. T., Dhooge, P. M., Glass, S. M., & Nimitz, J. S. (n.d.). *High-Performance, Low Environmental Impact Refrigerants*.

[16] Maryatt, B. W., & Smith, M. J. (n.d.). *Microbial Growth Control in the International Space Station Potable Water Dispenser*.

[17] *Bolt Shear Stress Calculator*. (2026, February 22). Firgelli Automations. https://www.firgelliauto.com/blogs/engineering-calculators/bolt-shear-stress-calculator

[18] *ASM Material Data Sheet Aluminum 6061-T6*. (n.d.). Retrieved March 3, 2026, from https://asm.matweb.com/search/specificmaterial.asp?bassnum=ma6061t6

[19] Budynas, R. G., & Nisbett, J. K. (2019). Shigley's mechanical engineering design (11th ed.). McGraw-Hill Education.

[20] *Disinfection Profiling and Benchmarking: Technical Guidance*. (n.d.). https://www.epa.gov/system/files/documents/2022-02/disprof_bench_3rules_final_508.pdf

[21] Maryatt, B. (2018, July 8–12). Lessons learned for the International Space Station potable water dispenser [Paper presentation]. 48th International Conference on Environmental Systems, Albuquerque, NM, United States. https://ices.space/wp-content/uploads/2024/09/Paper-Reference-List-by-Session-FINAL-PDF.pdf

[22] Leidos deploys Potable Water System to International Space Station | Leidos. (n.d.). Retrieved May 26, 2026, from https://www.leidos.com/insights/leidos-deploys-potable-water-system-international-space-station

[23] Toon, K., & Lovell, R. (2010). International Space Station United States On-orbit Segment Potable Water Dispenser On-orbit Functionality vs. Design. In 40th International Conference on Environmental Systems. American Institute of Aeronautics and Astronautics. https://doi.org/10.2514/6.2010-6250

[24] *Public Payload User Guide 2024 | Virgin Galactic*. (n.d.). Retrieved May 26, 2026, from https://bynder.virgingalactic.com/m/79e8c34fe3c4d35d/original/Public-Payload-User-Guide_May-2024.pdf

[25] Boyle, A. (2020, December 15). Ancient art of origami provides a pathway for building a better tank for rocket fuel. *GeekWire*. https://www.geekwire.com/2020/ancient-art-origami-provides-pathway-building-better-tank-rocket-fuel/

[26] Straub, J. E. I. I., Plumlee, D. K., Wallace, W. T., Alverson, J. T., Benoit, M. J., Gillispie, R. L., Hunter, D., Kuo, M., Rutz, J. A., Hudson, E. K., Loh, L. J., & Gazda, D. B. (2017). *ISS Potable Water Sampling and Chemical Analysis Results for 2016*. http://hdl.handle.net/2346/73099

[27] Westhoff Larner, K., McPhail, C., & Romero, C. (2022). *Optimization of a Deionization Bed for an Oxygen Generator Assembly for Exploration Missions*. https://hdl.handle.net/2346/89605

[28] Nadeau, M. L., Almengor, A., Muirhead, D., Ott, M., & Callahan, M. (2023). *To Biocide or not to Biocide? Exploring the "No Biocide" Option in Spacecraft Potable Water Systems*. https://hdl.handle.net/2346/94664

[29] Rector, T., Metselaar, C., Peyton, B., Steele, J., Michalek, W., Bowman, E., Wilson, M., Gazda, D., & Carter, L. (2014, July 13). *An Evaluation of Technology to Remove Problematic Organic Compounds from the International Space Station Potable Water*. International Conference on Environmental Systems (ICES). https://ntrs.nasa.gov/citations/20140012507

[30] Steele, J., Wilson, M., Makinen, J., & Ott, C. M. (2018, July 8). *Antimicrobials for Water Systems in Manned Spaceflight—Past, Present, and Future Applications and Challenges*. International Conference On Environmental Systems, Inc. https://ntrs.nasa.gov/citations/20180004666

[31] Rector, T., Peyton, B. M., Steele, J. W., Makinen, J., Bue, G. C., & Campbell, C. (2014, July 13). *Performance of Water Recirculation Loop Maintenance Components for the Advanced Spacesuit Water Membrane Evaporator*. American Society of Mechanical Engineers. https://ntrs.nasa.gov/citations/20140009382

[32] NASA, "International Space Station Potable Water Dispenser (PWD) Technical Specification Guidelines and Baseline Engineering Sizing Briefing Documents," Internal Reference Compilation Materials, 2025.

[33] Toon, K., & Lovell, R. (2010). *International Space Station United States On-orbit Segment Potable Water Dispenser On-orbit Functionality vs. Design*. Paper presented at the 40th International Conference on Environmental Systems, Barcelona, Spain. https://doi.org/10.2514/6.2010-6250

[34] *PCEC – Project Cost Estimating Capability—NASA*. (n.d.). Retrieved May 26, 2026, from https://www.nasa.gov/ocfo/ppc-corner/pcec-project-cost-estimating-capability/

Calculations

Heating Calculator Results

Setup

Water in coil	-->	Pipe Wall Thickness	-->	Heating Strips	-->	Insulation	-->	Ambient

Heating inputs

Symbol	Description	Value	Units	source
T_supply,h	Incoming water temperature	22.5	degC	NASA-STD-3001
T_coil,h,i	Initial coil water temperature	22.5	degC	
T_res,h,target	Target reservoir water temperature	22.5	degC	NASA-STD-3001
V_res,h,target	Hot reservoir target volume w/ 5% margin	0.63	L	https://www.nas
P_el,h	Electrical heater power	779	W	using outer later
eta_h	Heater efficiency	0.7	-	Janine
T_inf,h	Ambient temperature	22.5	degC	
h_i,h	Inner convection coefficient	500	W/m^2-K	Fundamentals o
h_o,amb,h	Outer convection coefficient to ambient	5	W/m^2-K	Fundamentals o
k_t,h	Tube thermal conductivity	167	W/m-K	aluminum 6061
d_i,h	Tube inner diameter	0.006	m	
d_o,h	Tube outer diameter	0.008	m	
L_h	Coil length	2	m	
R_t,c,h	Thermal contact resistance	0.000000635341	K/W	R=t/k*pi*d*L, Ka
t_ins,h	Heater-side insulation thickness	0.005	m	https://www.buy
k_ins,h	Heater-side insulation conductivity	0.014	W/m-K	https://www.buy
rho_w	Water density	998	kg/m^3	
c_p,w	Water specific heat	4184	J/kg-K	
Q_vol	Volumetric flow rate	500	mL/min	
m_dot_w	Mass flow rate	0.0083	kg/s	
t	time step	1	s	

Heating Derivations

Symbol	Description	Value	Units	Equation
A_i,h	Inner lateral surface area	0.03770	m^2	A_i,h = pi * d_i,h * L_h
A_o,h	Outer lateral surface area	0.05027	m^2	A_o,h = pi * d_o,h * L_h
V_coil,h	Coil water hold-up volume	0.05655	L	V_coil,h = 1000 * pi * d_i,h^2 / 4 * L_h
m_res,h, target	Reservoir mass	0.62874	kg	m_res,h, target = rho_w * V_res,h / 1000
m_coil,h	Coil water mass	0.05644	kg	m_coil,h = rho_w * pi * d_i,h^2 / 4 * L_h
P_h,eff	Effective heater power	545.300	W	P_h,eff = eta_h * P_el,h
R_t,conv,i,h	Inner convection resistance	0.05305	K/W	R_t,conv,i,h = 1 / (h_i,h * A_i,h)
R_t,cond,t,h	Tube-wall conduction resistance	0.00014	K/W	R_t,cond,t,h = ln(d_o,h / d_i,h) / (2 * pi * k_t,h * L_h)
R_t,c,h	Thermal contact resistance	0.00000	K/W	R_t,c,h = input contact resistance
R_t,w-s,h	Water-to-strip resistance	0.05319	K/W	R_t,w-s,h = R_t,conv,i,h + R_t,cond,t,h + R_t,c,h
R_t,conv,o,amb,h	Outer convection resistance to ambient (bare)	3.97887	K/W	R_t,conv,o,amb,h = 1 / (h_o,amb,h * A_o,h)
A_ins,o,h	Insulated outer area	0.11310	m^2	A_ins,o,h = pi * (d_o,h + 2 * t_ins,h) * L_h
R_t,cond,ins,h	Insulation conduction resistance	4.60941	K/W	R_t,cond,ins,h = ln((d_o,h + 2 * t_ins,h) / d_o,h) / (2 * pi * k_ins,h * L_h)
R_t,loss,amb,h	Total ambient-loss resistance	6.37780	K/W	R_t,loss,amb,h = R_t,cond,ins,h + 1 / (h_o,amb,h * A_ins,o,h)
T_s,h	Heater strip surface temperature	51.26427	C	T_s,h = (P_h,eff + T_coil,h / R_t,w-s,h + T_inf,h / R_t,loss,amb,h) / (1 / R_t,w-s,h + 1 / R_t,loss,amb,h)
q_h->w	Heat transferred from coil water to heater strip	540.7899	W	q_h->w = (T_s,h - T_coil,h) / R_t,w-s,h
q_loss->amb	Heat lost from heater strip to ambient	4.5101	W	q_loss,amb = (T_s,h - T_inf,h) / R_t,loss,amb,h

Heating with Time Plots (5 minutes)

Time, s	Time, min	m_res,h(t), kg	V_res,h(t), L	T_supply,h, C	T_coil,h, C	T_s,h, C	q_h->w, W	q_loss,amb, W	Heater check, W	dT_coil/dt, C/s	T_res,h, C
0.00	0.00	0.00000	0.00000	22.50	22.50000	51.26427	540.78994	4.51006	545.3	2.29026	
1.00	0.02	0.00830	0.00832	22.50	24.79026	53.53559	540.43381	4.86619	545.3	1.95192	24.79026
2.00	0.03	0.01660	0.01663	22.50	26.74217	55.47136	540.13029	5.16971	545.3	1.66356	25.76622
3.00	0.05	0.02490	0.02495	22.50	28.40574	57.12117	539.87161	5.42839	545.3	1.41781	26.64606
4.00	0.07	0.03320	0.03327	22.50	29.82355	58.52725	539.65115	5.64885	545.3	1.20836	27.44043
5.00	0.08	0.04150	0.04158	22.50	31.03190	59.72561	539.46325	5.83675	545.3	1.02985	28.15872
6.00	0.10	0.04980	0.04990	22.50	32.06175	60.74694	539.30311	5.99689	545.3	0.87771	28.80923
7.00	0.12	0.05810	0.05822	22.50	32.93946	61.61739	539.16663	6.13337	545.3	0.74805	29.39926
8.00	0.13	0.06640	0.06653	22.50	33.68751	62.35925	539.05031	6.24969	545.3	0.63754	29.93529
9.00	0.15	0.07470	0.07485	22.50	34.32504	62.99152	538.95118	6.34882	545.3	0.54336	30.42304
10.00	0.17	0.08300	0.08317	22.50	34.86840	63.53038	538.86669	6.43331	545.3	0.46309	30.86758
11.00	0.18	0.09130	0.09148	22.50	35.33148	63.98963	538.79468	6.50532	545.3	0.39467	31.27339
12.00	0.20	0.09960	0.09980	22.50	35.72616	64.38104	538.73331	6.56669	545.3	0.33637	31.64445
13.00	0.22	0.10790	0.10812	22.50	36.06253	64.71463	538.68101	6.61899	545.3	0.28668	31.98430
14.00	0.23	0.11620	0.11643	22.50	36.34921	64.99894	538.63643	6.66357	545.3	0.24433	32.29608
15.00	0.25	0.12450	0.12475	22.50	36.59354	65.24125	538.59844	6.70156	545.3	0.20823	32.58258
16.00	0.27	0.13280	0.13307	22.50	36.80177	65.44776	538.56606	6.73394	545.3	0.17747	32.84628

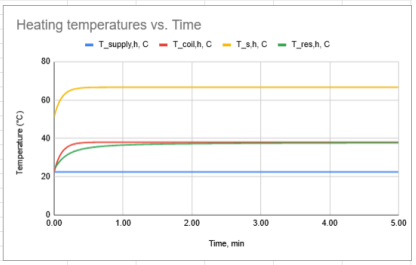

Cooling Calculator Results

Setup

Water source	-->	Parallel water channels	-->	Shared wall / closed-loop refrigerant	-->	Outer insulation around assembly	-->	Ambient

Cooling Heat Transfer

Cooling goes to refrigerant or amb	q_w->s + q_amb->s = q_s->ref
Cold channel surface temperature	T_s,c = (T_tube/R_t,w-s,c + T_ref,c/R_t,conv,o,ref,c + T_inf,c/R_t,amb-s,c) / (1/R_t,w-s,c + 1/R_t,conv,o,ref,c + 1/R_t,amb-s,c)
Cooling to water	q_w->s = (T_tube - T_s,c) / R_t,w-s,c
Bladder fill average	T_bladd,avg is the collected average of cooled outlet water; V_bladd,c(t) is calculated from Q_vol over time until the target volume is reached
Channel energy balance, cooling	m_tube c_p dT_tube/dt = -q_w->s + m_dot c_p (T_source - T_tube)

Cooling inputs

Symbol	Description	Value	Units
T_source,c	Source water temperature	22.5	degC
T_tube,c,i	Initial water in cooling channels	22.5	degC
T_bladd,c,target	Target bladder water temperature	10	degC
V_bladd,c	Cold bladder target volume	0.5	L
T_inf,c	Ambient temperature	22.5	degC
T_ref,c	Refrigerant-side boundary temperature	5	degC
h_i,c	Water-side convection coefficient	500	W/m^2-K
h_ref,c	Refrigerant-side convection coefficient	100	W/m^2-K
h_amb,c	Ambient convection coefficient	5	W/m^2-K
k_wall,c	Shared wall conductivity	16	W/m-K
A_ch,w,c	Area of one water channel	0.0000282743	m^2
D_h,w,c	Hydraulic diameter of one water channel	0.006	m
L_c	Single-channel length	0.5	m
N_w,ch,c	Parallel water channels	6	-
f_contact,c	Effective refrigerant contact perimeter fraction	1	-
P_ins,o,c	Outer insulated perimeter of assembly	0.05655	m
t_wall,c	Water/refrigerant wall thickness	0.001	m
t_ins,c	Insulation thickness	0.005	m
k_ins,c	Insulation conductivity	0.04	W/m-K
rho_w	Water density	998	kg/m^3
c_p,w	Water specific heat	4184	J/kg-K
Q_vol	Water flow rate into bladder	500	mL/min
t	Time step	1	s

Cooling derived quantities

Symbol	Description	Value	Units	Equation
A_ht,w,c	Water-side heat-transfer area	0.05655	m^2	A_ht,w,c = N_w,ch,c * f_contact,c * (4 * A_ch,w,c / D_h,w,c) * L_c
A_ht,ref,c	Refrigerant contact area	0.05655	m^2	A_ht,ref,c = A_ht,w,c
V_tube,c	Tube water hold-up volume	0.08482	L	V_tube,c = 1000 * A_ch,w,c * N_w,ch,c * L_c
m_bladd,c	Bladder water mass	0.49900	kg	m_bladd,c = rho_w * V_bladd,c / 1000
m_tube,c	Tube water mass	0.08465	kg	m_tube,c = rho_w * A_ch,w,c * N_w,ch,c * L_c
m_dot_w	Mass flow rate	0.00832	kg/s	m_dot_w = rho_w * Q_vol / 1e6 / 60
R_t,conv,i,c	Water-side convection resistance	0.03537	K/W	R_t,conv,i,c = 1 / (h_i,c * A_ht,w,c)
R_t,cond,wall,c	Shared wall conduction resistance	0.00111	K/W	R_t,cond,wall,c = t_wall,c / (k_wall,c * A_ht,w,c)
R_t,w-s,c	Water-to-surface resistance	0.03647	K/W	R_t,w-s,c = R_t,conv,i,c + R_t,cond,wall,c
R_t,conv,o,ref,c	Refrigerant-side convection resistance	0.17684	K/W	R_t,conv,o,ref,c = 1 / (h_ref,c * A_ht,ref,c)
A_ins,o,c	Insulated outer area	0.02828	m^2	A_ins,o,c = P_ins,o,c * L_c
R_t,conv,o,amb,c	Ambient convection resistance	7.07339	K/W	R_t,conv,o,amb,c = 1 / (h_amb,c * A_ins,o,c)
R_t,cond,ins,c	Insulation conduction resistance	4.42087	K/W	R_t,cond,ins,c = t_ins,c / (k_ins,c * A_ins,o,c)
R_t,amb-s,c	Total ambient-to-surface resistance	11.49425	K/W	R_t,amb-s,c = R_t,conv,o,amb,c + R_t,cond,ins,c
T_s,c	Initial cold surface temperature	19.5156	C	T_s,c = weighted node temperature
q_w->s	Initial heat removed from water	81.8242	W	q_w->s = (T_tube,c - T_s,c) / R_t,w-s,c
q_amb->s	Initial ambient heat leak to cold surface	0.2596	W	q_amb->s = (T_inf,c - T_s,c) / R_t,amb-s,c
q_s->ref	Initial heat rejected to refrigerant	82.08381423	W	q_s->ref = (T_s,c - T_ref,c) / R_t,conv,o,ref,c
t_fill,bladd,c	Bladder fill time	60	s	t_fill,bladd,c = V_bladd,c / (Q_vol / 1000 / 60)
A_flow,total,c	Total water flow area	0.0001696458	m^2	A_flow,total,c = A_ch,w,c * N_w,ch,c
A_ht_per_m,c	Heat-transfer area per meter	0.1130972	m^2/m	A_ht_per_m,c = N_w,ch,c * f_contact,c * (4 * A_ch,w,c / D_h,w,c)
T_bladd,final,c	Final bladder average temperature	20.7050	degC	T_bladd,final,c = LOOKUP(t_fill, time, T_bladd,avg,c)
Target reached?	Target check	No - increase L_	-	IF(T_bladd,final,c <= T_bladd,c,target)

Cooling with Time Plots

Time, s	Time, min	T_bladd,avg,c, C	T_tube/outlet,c, C	T_s,c, C	q_w->s, W	q_amb->s, W	q_s->ref, W	V_bladd,c, L	Bladder filling?	dT_tube/dt, C/s
0.0000	0.0000	22.5000	22.5000	19.5156	81.8242	0.2596	82.0838	0.0000	Filling	-0.2310
1.0000	0.0167	22.2690	22.2690	19.3246	80.7274	0.2763	81.0036	0.0083	Filling	-0.2052
2.0000	0.0333	22.1664	22.0638	19.1549	79.7531	0.2910	80.0441	0.0167	Filling	-0.1823
3.0000	0.0500	22.0714	21.8814	19.0042	78.8875	0.3041	79.1917	0.0250	Filling	-0.1620
4.0000	0.0667	21.9834	21.7195	18.8703	78.1186	0.3158	78.4344	0.0333	Filling	-0.1439
5.0000	0.0833	21.9019	21.5756	18.7513	77.4355	0.3261	77.7617	0.0417	Filling	-0.1278
6.0000	0.1000	21.8262	21.4478	18.6456	76.8287	0.3353	77.1641	0.0500	Filling	-0.1135
7.0000	0.1167	21.7559	21.3343	18.5517	76.2897	0.3435	76.6332	0.0583	Filling	-0.1009
8.0000	0.1333	21.6906	21.2334	18.4683	75.8108	0.3508	76.1616	0.0667	Filling	-0.0896
9.0000	0.1500	21.6298	21.1438	18.3943	75.3854	0.3572	75.7426	0.0750	Filling	-0.0796
10.0000	0.1667	21.5733	21.0642	18.3284	75.0075	0.3629	75.3704	0.0833	Filling	-0.0707
11.0000	0.1833	21.5206	20.9935	18.2700	74.6718	0.3680	75.0398	0.0917	Filling	-0.0628
12.0000	0.2000	21.4714	20.9307	18.2180	74.3736	0.3725	74.7461	0.1000	Filling	-0.0558
13.0000	0.2167	21.4255	20.8749	18.1719	74.1086	0.3765	74.4852	0.1083	Filling	-0.0496
14.0000	0.2333	21.3826	20.8253	18.1309	73.8733	0.3801	74.2534	0.1167	Filling	-0.0440
15.0000	0.2500	21.3425	20.7812	18.0945	73.6642	0.3833	74.0475	0.1250	Filling	-0.0391
16.0000	0.2667	21.3050	20.7421	18.0621	73.4785	0.3861	73.8645	0.1333	Filling	-0.0348

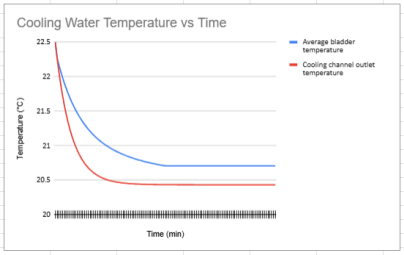

Heating and Cooling Calculator Breakdown

1 Purpose of the Calculator

This calculator models the transient heating behavior of a potable water dispensing system using a heated tube coil and reservoir. The spreadsheet estimates:

- Coil water temperature
- Reservoir water temperature
- Heater surface temperature
- Heat transfer into the water
- Heat losses to ambient
- Reservoir mass and volume accumulation

The spreadsheet uses thermal resistance methods, transient energy balances, and explicit time stepping to propagate the solution through time.

2 User Inputs

The primary inputs are entered under the "Heating Inputs" section of the spreadsheet.

Heating inputs				
Symbol	Description		Value	Units
T_supply,h	Incoming water temperature		22.5	degC
T_coil,h,i	Initial coil water temperature		22.5	degC
T_res,h,target	Target reservoir water temperature		22.5	degC
V_res,h,target	Hot reservoir target volume	w/ 5% margin	0.63	L
P_el,h	Electrical heater power		560	W
eta_h	Heater efficiency		0.7	-
T_inf,h	Ambient temperature		22.5	degC
h_i,h	Inner convection coefficient		500	W/m^2-K
h_o,amb,h	Outer convection coefficient to ambient		5	W/m^2-K
k_t,h	Tube thermal conductivity		167	W/m-K
d_i,h	Coil inner diameter		0.006	m
d_o,h	Coil outer diameter		0.008	m
L_h	Coil length		2	m
R_t,c,h	Thermal contact resistance		0.000000635349	K/W
t_ins,h	Heater-side insulation thickness		0.005	m
k_ins,h	Heater-side insulation conductivity		0.014	W/m-K
rho_w	Water density		998	kg/m^3
c_p,w	Water specific heat		4184	J/kg-K
Q_vol	Volumetric flow rate		500	mL/min
m_dot_w	Mass flow rate		0.0083	kg/s
t	time step		1	s

Figure 1: Heating Inputs Table

3 Geometric Properties

The internal wetted area of the tube is:

$$A_{i,h} = \pi d_{i,h} L_h$$

Substituting values:

$$A_{i,h} = \pi(0.006)(2) = 0.0377 \ m^2$$

The external tube area is:

$$A_{o,h} = \pi d_{o,h} L_h$$

Substituting values:

$$A_{o,h} = \pi(0.008)(2) = 0.0503 \ m^2$$

The internal fluid volume of the coil is:

$$V_{coil,h} = 1000 \left(\frac{\pi d_{i,h}^2}{4} L_h \right)$$

Substituting values:

$$V_{coil,h} = 1000 \left(\frac{\pi(0.006)^2}{4}(2) \right) = 0.0565 \ L$$

4 Fluid Mass Calculations

The target heated reservoir water mass is:

$$m_{res,h,target} = \rho_w \frac{V_{res,h,target}}{1000}$$

Substituting values:

$$m_{res,h,target} = 998 \frac{1}{1000} = 0.998 \ kg$$

The mass of water inside the coil is:

$$m_{coil,h} = \rho_w \left(\frac{\pi d_{i,h}^2}{4} L_h \right)$$

Substituting values:

$$m_{coil,h} = 998 \left(\frac{\pi(0.006)^2}{4}(2) \right) = 0.0564 \ kg$$

5 Effective Heater Power

The effective thermal power delivered by the heater is:

$$P_{h,eff} = \eta_h P_{el,h}$$

Substituting values:

$$P_{h,eff} = 0.7(560) = 392\ W$$

6 Thermal Resistance Network

Heat transfer within the system occurs radially through a set of thermal resistances. The resistances are listed in the order they occur from the center of the flowing water outward toward the ambient surroundings.

The full thermal path is:

Water → Internal Convection → Tube Wall Conduction → Thermal Contact → Insulation Conduction → Ambier

6.1 Internal Convection Resistance

The first resistance occurs between the flowing water and the inner tube wall.

The internal convection resistance is:

$$R_{t,conv,i,h} = \frac{1}{h_{i,h} A_{i,h}}$$

Substituting values:

$$R_{t,conv,i,h} = \frac{1}{500(0.0377)} = 0.0530\ K/W$$

6.2 Tube Wall Conduction Resistance

After heat reaches the inner tube wall, it conducts radially through the tube material.

The cylindrical conduction resistance of the tube wall is:

$$R_{t,cond,t,h} = \frac{\ln(d_{o,h}/d_{i,h})}{2\pi k_{t,h} L_h}$$

Substituting values:

$$R_{t,cond,t,h} = \frac{\ln(0.008/0.006)}{2\pi(167)(2)} = 1.37 \times 10^{-4}\ K/W$$

6.3 Thermal Contact Resistance

After conduction through the tube wall, heat passes through the interface between the heater and tube surface.

The thermal contact resistance is entered directly as:

$$R_{t,c,h} = \text{user-defined input} = 0.0000006353490742 for Kapton$$

This resistance accounts for imperfect surface contact, air gaps, surface roughness, clamping force, and thermal interface materials.

6.4 Insulation Conduction Resistance

Heat leaving the heater assembly then conducts through the external insulation layer.

The external insulation area is:

$$A_{ins,o,h} = \pi(d_{o,h} + 2t_{ins,h})L_h$$

The insulation conduction resistance is:

$$R_{t,cond,ins,h} = \frac{\ln((d_{o,h} + 2t_{ins,h})/d_{o,h})}{2\pi k_{ins,h} L_h}$$

6.5 Ambient Convection Resistance

The final resistance occurs between the outer insulation surface and the surrounding air.

The ambient convection resistance is:

$$R_{t,conv,o,amb,h} = \frac{1}{h_{o,amb,h} A_{ins,o,h}}$$

6.6 Total Water-Side Resistance

The total resistance between the heater surface and the water is:

$$R_{t,w-s,h} = R_{t,conv,i,h} + R_{t,cond,t,h} + R_{t,c,h}$$

6.7 Total Ambient Heat Loss Resistance

The total resistance between the heater surface and the ambient surroundings is:

$$R_{t,loss,amb,h} = R_{t,cond,ins,h} + R_{t,conv,o,amb,h}$$

7 Heater Surface Temperature

The heater surface temperature is calculated using a thermal resistance balance.

At the heater surface:

$$P_{h,eff} = \dot{Q}_{h\to w} + \dot{Q}_{loss,amb}$$

Substituting resistance relations:

$$P_{h,eff} = \frac{T_{s,h} - T_{coil,h}}{R_{t,w-s,h}} + \frac{T_{s,h} - T_{\infty,h}}{R_{t,loss,amb,h}}$$

Solving for heater surface temperature:

$$T_{s,h} = \frac{P_{h,eff} + \frac{T_{coil,h}}{R_{t,w-s,h}} + \frac{T_{\infty,h}}{R_{t,loss,amb,h}}}{\frac{1}{R_{t,w-s,h}} + \frac{1}{R_{t,loss,amb,h}}}$$

8 Heat Transfer Into the Water

The heat transfer rate into the water is:

$$\dot{Q}_{h\to w} = \frac{T_{s,h} - T_{coil,h}}{R_{t,w-s,h}}$$

This quantity is recalculated every timestep because the heater surface temperature and coil water temperature are updated every row.

9 Heat Loss to Ambient

The ambient heat loss is:

$$\dot{Q}_{loss,amb} = \frac{T_{s,h} - T_{\infty,h}}{R_{t,loss,amb,h}}$$

This quantity is recalculated every timestep because the heater surface temperature changes over time.

10 Energy Balance Verification

The spreadsheet verifies conservation of energy using:

$$P_{h,eff} = \dot{Q}_{h\to w} + \dot{Q}_{loss,amb}$$

Minor differences occur due to numerical rounding.

11 Transient Coil Heating Equation

The transient energy balance on the coil water control volume is:

$$m_{coil,h} c_p \frac{dT_{coil,h}}{dt} = \dot{Q}_{h\to w} + \dot{m} c_p (T_{supply,h} - T_{coil,h})$$

Solving for the temperature rate of change:

$$\frac{dT_{coil,h}}{dt} = \frac{\dot{Q}_{h\to w} + \dot{m} c_p (T_{supply,h} - T_{coil,h})}{m_{coil,h} c_p}$$

12 Euler Time Stepping

The spreadsheet uses explicit Euler integration.

Each spreadsheet row represents one timestep:

$$t_{n+1} = t_n + \Delta t$$

where:

$$\Delta t = 1 \ s$$

The coil temperature is updated using:

$$T_{coil,h}(t + \Delta t) = T_{coil,h}(t) + \frac{dT_{coil,h}}{dt}\Delta t$$

This process repeats for every spreadsheet row.

13 Reservoir Mass and Volume Updates

The reservoir mass increases according to:

$$m_{res,h}(t + \Delta t) = m_{res,h}(t) + \dot{m}\Delta t$$

The reservoir volume is then calculated from density:

$$V_{res,h} = \frac{1000 m_{res,h}}{\rho_w}$$

14 Reservoir Temperature Update

The reservoir temperature is calculated using a mass-weighted mixing relation:

$$T_{res,h}(t + \Delta t) = \frac{m_{old}T_{old} + m_{new}T_{coil,h}}{m_{total}}$$

This assumes perfect mixing inside the reservoir.

15 Transient Plot Generation

The spreadsheet generates plots by recalculating all temperatures and heat transfer quantities at every timestep.

The primary transient plots include:

- Coil water temperature vs. time
- Reservoir temperature vs. time
- Heater surface temperature vs. time
- Heat transfer into water vs. time
- Ambient heat loss vs. time

- Reservoir mass vs. time
- Reservoir volume vs. time

Each plotted value is obtained from the updated equations in the corresponding spreadsheet row.

15.1 Coil Water Temperature Plot

The coil water temperature plot shows the calculated temperature of the water inside the heating coil at each timestep.

The plotted values come from:

$$T_{coil,h}(t + \Delta t) = T_{coil,h}(t) + \frac{dT_{coil,h}}{dt}\Delta t$$

15.2 Reservoir Temperature Plot

The reservoir temperature plot shows the mixed temperature of the water collected in the reservoir.

The plotted values come from:

$$T_{res,h}(t + \Delta t) = \frac{m_{old}T_{old} + m_{new}T_{coil,h}}{m_{total}}$$

15.3 Heater Surface Temperature Plot

The heater surface temperature plot shows the calculated surface temperature from the resistance balance.

The plotted values come from:

$$T_{s,h} = \frac{P_{h,eff} + \frac{T_{coil,h}}{R_{t,w-s,h}} + \frac{T_{\infty,h}}{R_{t,loss,amb,h}}}{\frac{1}{R_{t,w-s,h}} + \frac{1}{R_{t,loss,amb,h}}}$$

15.4 Heat Transfer Into Water Plot

The heat transfer into water plot shows the instantaneous heating rate of the coil water.

The plotted values come from:

$$\dot{Q}_{h\to w} = \frac{T_{s,h} - T_{coil,h}}{R_{t,w-s,h}}$$

15.5 Ambient Heat Loss Plot

The ambient heat loss plot shows the instantaneous heat loss from the system to ambient air.

The plotted values come from:

$$\dot{Q}_{loss,amb} = \frac{T_{s,h} - T_{\infty,h}}{R_{t,loss,amb,h}}$$

15.6 Reservoir Mass and Volume Plots

The reservoir mass and volume plots show the accumulation of heated water in the reservoir.

The plotted mass values come from:

$$m_{res,h}(t + \Delta t) = m_{res,h}(t) + \dot{m}\Delta t$$

The plotted volume values come from:

$$V_{res,h} = \frac{1000 m_{res,h}}{\rho_w}$$

16 Important Assumptions

- Constant water properties
- Constant material properties
- Uniform coil temperature
- Perfect reservoir mixing
- One-dimensional radial heat transfer
- Negligible radiation heat transfer
- Constant heater efficiency

17 Conclusion

This spreadsheet models transient heating behavior using:

- Convection
- Conduction
- Thermal resistance methods
- Energy conservation
- Explicit Euler time stepping
- Numerical transient updates

The calculator provides a transient estimate of water heating performance for a potable water dispensing system.

18 Water Cooler Calculator

The cooling portion of the spreadsheet models the transient cooling behavior of water flowing through a multichannel tube. In this system, room-temperature source water is pushed through water channels in a multichannel tube. The neighboring channels contain closed-loop refrigerant, which removes heat from the water through the shared channel walls. After passing through the cooling length, the cooled water collects in an insulated bladder. The bladder is then emptied through a nozzle after it reaches the desired fill volume.

Unlike the heating reservoir model, the cold bladder is assumed to be initially empty. Therefore, the bladder temperature is not an initial water temperature. Instead, it is calculated as the running average temperature of the cooled water exiting the multichannel cooling section.

The cooling calculator estimates:

- Water temperature inside the cooling channels
- Effective cold surface temperature
- Heat removed from the water
- Ambient heat leak into the cold section
- Heat rejected to the refrigerant
- Bladder fill volume over time
- Average temperature of the collected bladder water

19 Cooling System Setup

The physical cooling path is modeled as:

Source Water → Multichannel Water Passages → Shared Tube Wall → Closed-Loop Refrigerant Channels → Insu

The thermal resistance path is modeled as:

Water → Water-Side Convection → Shared Wall Conduction → Refrigerant-Side Convection → Refrigerant

Ambient heat leak is also included through the insulation surrounding the multichannel tube and refrigerant section:

Ambient → Ambient Convection → Insulation Conduction → Cold Surface

20 Cooling Inputs

The main cooling inputs are entered under the "Cooling Inputs" section of the spreadsheet.

Important cooling inputs include:

- Source water temperature, $T_{source,c}$

- Initial water temperature in the cooling channels, $T_{tube,c,i}$
- Target bladder water temperature, $T_{bladd,c,target}$
- Cold bladder target volume, $V_{bladd,c,target}$
- Refrigerant-side boundary temperature, $T_{ref,c}$
- Area of one water channel, $A_{ch,w,c}$
- Hydraulic diameter of one water channel, $D_{h,w,c}$
- Number of parallel water channels, $N_{w,ch,c}$
- Single-channel length, L_c
- Water-side convection coefficient, $h_{i,c}$
- Refrigerant-side convection coefficient, $h_{ref,c}$
- Ambient convection coefficient, $h_{amb,c}$
- Wall conductivity, $k_{wall,c}$
- Insulation conductivity, $k_{ins,c}$
- Volumetric flow rate, Q_{vol}, which sets the bladder fill volume over time

21 Multichannel Geometry

The total water flow area is calculated from the area of one water channel and the number of parallel water channels:

$$A_{flow,total,c} = N_{w,ch,c} A_{ch,w,c}$$

The water volume inside the cooling channels is:

$$V_{tube,c} = 1000 A_{flow,total,c} L_c$$

where the factor of 1000 converts cubic meters to liters.
The mass of water inside the cooling channels is:

$$m_{tube,c} = \rho_w A_{flow,total,c} L_c$$

22 Hydraulic Diameter

For non-circular cooling channels, the hydraulic diameter is used instead of the circular tube diameter. The hydraulic diameter is:

$$D_h = \frac{4A_c}{P_w}$$

where:

A_c = cross-sectional area of one channel

P_w = wetted perimeter of one channel

The hydraulic diameter allows the spreadsheet to use pipe-flow style heat transfer relations for a non-circular channel.

23 Cooling Heat Transfer Area

The effective water-side heat transfer area is based on the hydraulic diameter, channel length, and number of water channels:

$$A_{w,c} = N_{w,ch,c}\pi D_{h,w,c}L_c$$

If only part of the water channel perimeter is effectively exposed to the neighboring refrigerant channels, a contact correction factor may be applied:

$$A_{contact,c} = f_{contact,c}A_{w,c}$$

where $f_{contact,c}$ is the effective refrigerant contact perimeter fraction.

24 Bladder Fill Volume Over Time

The bladder is assumed to start empty. Instead of assuming that the bladder is already filled, the spreadsheet uses the volumetric flow rate to calculate how much cooled water has entered the bladder at each timestep.

The volumetric flow rate is entered as:

$$Q_{vol} = 500\ mL/min$$

This is converted to liters per second as:

$$Q_{vol,L/s} = \frac{Q_{vol}}{1000(60)}$$

Substituting values:

$$Q_{vol,L/s} = \frac{500}{1000(60)} = 0.00833\ L/s$$

The bladder fill volume at each timestep is:

$$V_{bladd,c}(t) = Q_{vol,L/s}t$$

To prevent the calculated bladder volume from exceeding the target bladder volume, the spreadsheet uses:

$$V_{bladd,c}(t) = \min\left(V_{bladd,c,target}, Q_{vol,L/s}t\right)$$

where:

$$V_{bladd,c,target} = \text{desired final bladder volume}$$

This means the bladder volume increases linearly with time until the target fill volume is reached. For example, if:

$$V_{bladd,c,target} = 0.5\ L$$

and:

$$Q_{vol} = 500\ mL/min = 0.5\ L/min$$

then the bladder fill time is:

$$t_{fill} = \frac{V_{bladd,c,target}}{Q_{vol}}$$

$$t_{fill} = \frac{0.5\ L}{0.5\ L/min} = 1\ min = 60\ s$$

The 60 second fill time is not an optimization result. It comes directly from the selected bladder volume and volumetric flow rate.

25 Cooling Thermal Resistance Network

Heat is removed from the water by passing through the water-side convection resistance, wall conduction resistance, and refrigerant-side convection resistance.

25.1 Water-Side Convection Resistance

The water-side convection resistance is:

$$R_{t,conv,i,c} = \frac{1}{h_{i,c} A_{contact,c}}$$

25.2 Shared Wall Conduction Resistance

The conduction resistance through the wall between the water and refrigerant channels is approximated as:

$$R_{t,cond,wall,c} = \frac{t_{wall,c}}{k_{wall,c} A_{contact,c}}$$

25.3 Water-to-Surface Resistance

The total resistance between the water and the cold surface is:

$$R_{t,w-s,c} = R_{t,conv,i,c} + R_{t,cond,wall,c}$$

25.4 Refrigerant-Side Convection Resistance

The refrigerant-side convection resistance is:

$$R_{t,conv,ref,c} = \frac{1}{h_{ref,c} A_{contact,c}}$$

25.5 Ambient Heat Leak Resistance

The ambient heat leak enters through the insulation surrounding the cold assembly.

The insulated outer area is:

$$A_{ins,o,c} = P_{ins,o,c} L_c$$

The insulation conduction resistance is approximated as:

$$R_{t,cond,ins,c} = \frac{t_{ins,c}}{k_{ins,c} A_{ins,o,c}}$$

The ambient convection resistance is:

$$R_{t,conv,amb,c} = \frac{1}{h_{amb,c} A_{ins,o,c}}$$

The total ambient-to-surface resistance is:

$$R_{t,amb-s,c} = R_{t,cond,ins,c} + R_{t,conv,amb,c}$$

26 Cold Surface Temperature

The cold surface temperature is calculated from a thermal resistance balance between the water, refrigerant, and ambient surroundings.

At the cold surface:

$$\dot{Q}_{w \to s} + \dot{Q}_{amb \to s} = \dot{Q}_{s \to ref}$$

Using the resistance relations:

$$\frac{T_{tube,c} - T_{s,c}}{R_{t,w-s,c}} + \frac{T_{\infty,c} - T_{s,c}}{R_{t,amb-s,c}} = \frac{T_{s,c} - T_{ref,c}}{R_{t,conv,ref,c}}$$

Solving for the cold surface temperature:

$$T_{s,c} = \frac{\frac{T_{tube,c}}{R_{t,w-s,c}} + \frac{T_{ref,c}}{R_{t,conv,ref,c}} + \frac{T_{\infty,c}}{R_{t,amb-s,c}}}{\frac{1}{R_{t,w-s,c}} + \frac{1}{R_{t,conv,ref,c}} + \frac{1}{R_{t,amb-s,c}}}$$

27 Heat Removed From the Water

The heat removed from the water is:

$$\dot{Q}_{w \to s} = \frac{T_{tube,c} - T_{s,c}}{R_{t,w-s,c}}$$

This value is positive when heat leaves the water and moves into the colder surface.

28 Ambient Heat Leak

The ambient heat leak into the cold section is:

$$\dot{Q}_{amb\to s} = \frac{T_{\infty,c} - T_{s,c}}{R_{t,amb-s,c}}$$

This is unwanted heat gain from the surrounding room-temperature air.

29 Heat Rejected to the Refrigerant

The heat rejected to the refrigerant is:

$$\dot{Q}_{s\to ref} = \frac{T_{s,c} - T_{ref,c}}{R_{t,conv,ref,c}}$$

For energy balance consistency:

$$\dot{Q}_{s\to ref} \approx \dot{Q}_{w\to s} + \dot{Q}_{amb\to s}$$

Small differences may occur because of spreadsheet rounding.

30 Transient Cooling Channel Equation

The cooling channel is modeled as a lumped water control volume with source water flowing in and cooled water flowing out.

The transient energy balance is:

$$m_{tube,c}c_p\frac{dT_{tube,c}}{dt} = -\dot{Q}_{w\to s} + \dot{m}_w c_p\left(T_{source,c} - T_{tube,c}\right)$$

Solving for the rate of temperature change:

$$\frac{dT_{tube,c}}{dt} = \frac{-\dot{Q}_{w\to s} + \dot{m}_w c_p\left(T_{source,c} - T_{tube,c}\right)}{m_{tube,c}c_p}$$

The negative sign on $\dot{Q}_{w\to s}$ indicates that heat is being removed from the water.

31 Euler Time Stepping for Cooling

The spreadsheet uses explicit Euler integration.

Each row advances by one timestep:

$$t_{n+1} = t_n + \Delta t$$

The cooling channel water temperature is updated using:

$$T_{tube,c}(t+\Delta t) = T_{tube,c}(t) + \frac{dT_{tube,c}}{dt}\Delta t$$

This updated cooling channel temperature is then used in the next row to recalculate the cold surface temperature and heat transfer rates.

32 Bladder Mass Accumulation

After the bladder fill volume is calculated, the collected water mass is calculated using the water density:

$$m_{bladd,c}(t) = \rho_w \frac{V_{bladd,c}(t)}{1000}$$

where $V_{bladd,c}$ is in liters.
The target bladder mass is:

$$m_{bladd,c,target} = \rho_w \frac{V_{bladd,c,target}}{1000}$$

The bladder is considered filling while:

$$V_{bladd,c}(t) < V_{bladd,c,target}$$

Once:

$$V_{bladd,c}(t) = V_{bladd,c,target}$$

the bladder is considered full.

33 Bladder Temperature Update

The bladder temperature is calculated as the running average of the cooled outlet water entering the bladder. Since the bladder starts empty, the first water entering the bladder defines the initial collected water temperature.

At each timestep, the new volume of water entering the bladder is:

$$\Delta V_{bladd,c} = Q_{vol,L/s} \Delta t$$

The corresponding new mass of water is:

$$m_{new} = \rho_w \frac{\Delta V_{bladd,c}}{1000}$$

The bladder temperature is updated using a mass-weighted mixing relation:

$$T_{bladd,c}(t + \Delta t) = \frac{m_{old} T_{old} + m_{new} T_{tube,c}}{m_{old} + m_{new}}$$

where:

$$T_{tube,c} = \text{cooling channel outlet temperature}$$

This assumes that the water entering the bladder has the same temperature as the outlet water from the multichannel cooling section.

Once the target bladder volume is reached, the calculator holds the bladder at the target fill volume.

34 Cooling Time Table

The cooling time table calculates all transient quantities at each timestep.

The main columns include:

- Time in seconds
- Time in minutes
- Average bladder water temperature
- Cooling channel outlet temperature
- Cold surface temperature
- Heat removed from water
- Ambient heat leak
- Heat rejected to refrigerant
- Bladder fill volume
- Bladder fill status
- Rate of change of cooling channel temperature

The most important design outputs are the average bladder temperature and the bladder fill volume. Together, these show whether the system can collect the desired volume of water below the target temperature before release through the nozzle.

35 Cooling Plot Generation

The spreadsheet generates plots by recalculating temperatures, heat transfer rates, and bladder fill volume at every timestep.

The primary cooling plots include:

- Cooling channel outlet temperature vs. time
- Average bladder temperature vs. time
- Cold surface temperature vs. time
- Heat removed from water vs. time
- Ambient heat leak vs. time
- Heat rejected to refrigerant vs. time
- Bladder fill volume vs. time

35.1 Cooling Channel Temperature Plot

The cooling channel temperature plot shows the water temperature inside the cooling channels at each timestep.

The plotted values come from:

$$T_{tube,c}(t + \Delta t) = T_{tube,c}(t) + \frac{dT_{tube,c}}{dt}\Delta t$$

35.2 Bladder Temperature Plot

The bladder temperature plot shows the average temperature of the water collected in the bladder.

The plotted values come from:

$$T_{bladd,c}(t + \Delta t) = \frac{m_{old}T_{old} + m_{new}T_{tube,c}}{m_{old} + m_{new}}$$

35.3 Cold Surface Temperature Plot

The cold surface temperature plot shows the effective surface temperature between the water channels, refrigerant channels, and ambient heat leak.

The plotted values come from:

$$T_{s,c} = \frac{\frac{T_{tube,c}}{R_{t,w-s,c}} + \frac{T_{ref,c}}{R_{t,conv,ref,c}} + \frac{T_{\infty,c}}{R_{t,amb-s,c}}}{\frac{1}{R_{t,w-s,c}} + \frac{1}{R_{t,conv,ref,c}} + \frac{1}{R_{t,amb-s,c}}}$$

35.4 Heat Removed From Water Plot

The heat removed from water plot shows the instantaneous cooling rate of the water.

The plotted values come from:

$$\dot{Q}_{w\to s} = \frac{T_{tube,c} - T_{s,c}}{R_{t,w-s,c}}$$

35.5 Ambient Heat Leak Plot

The ambient heat leak plot shows the instantaneous heat gain from the surrounding air into the insulated cold section.

The plotted values come from:

$$\dot{Q}_{amb\to s} = \frac{T_{\infty,c} - T_{s,c}}{R_{t,amb-s,c}}$$

35.6 Refrigerant Heat Rejection Plot

The refrigerant heat rejection plot shows the heat that must be carried away by the refrigerant loop.

The plotted values come from:

$$\dot{Q}_{s\to ref} = \frac{T_{s,c} - T_{ref,c}}{R_{t,conv,ref,c}}$$

35.7 Bladder Fill Volume Plot

The bladder fill volume plot shows how much cooled water has collected in the bladder over time. The plotted values come from:

$$V_{bladd,c}(t) = \min\left(V_{bladd,c,target}, Q_{vol,L/s}t\right)$$

This plot is important because it shows when the bladder reaches the desired release volume.

36 Important Cooling Assumptions

- The bladder starts empty.
- The bladder fill volume is calculated from the volumetric flow rate.
- The entered flow rate is $Q_{vol} = 500\ mL/min$ unless changed by the user.
- The bladder temperature is the mass-weighted average of water entering from the cooling channels.
- The cooling channel is modeled as a lumped control volume.
- The outlet temperature is approximated as the cooling channel water temperature.
- Water properties are constant.
- Refrigerant-side boundary temperature is constant.
- Refrigerant-side convection coefficient is constant.
- Ambient temperature is constant.
- Heat transfer is approximated as one-dimensional through an effective contact area.
- Radiation heat transfer is neglected.
- The bladder is insulated after collection.
- The nozzle release occurs after the bladder reaches the desired fill volume.

37 Cooling Calculator Conclusion

The water cooler calculator models the transient cooling of source water through a multichannel tube and the collection of that cooled water in an initially empty insulated bladder. The model uses:

- Multichannel heat transfer area
- Hydraulic diameter
- Thermal resistance methods
- Water-to-refrigerant heat transfer

- Ambient heat leak through insulation
- Transient energy balances
- Explicit Euler time stepping
- Volumetric bladder fill calculation
- Mass-weighted bladder temperature accumulation

The calculator can be used to estimate whether a selected channel length, number of channels, refrigerant boundary temperature, and flow rate are sufficient to fill the bladder with water below the target temperature.

Decontamination Breakdown

Decontamination Breakdown

Decontamination subsystem requirements

- Consumable Iodine level < 0.2 ppm [2, 3]
- Consumable CFU/mL level < 50 CFU/mL [2, 3]

Purpose of this study:

1. Compute and define system and hardware requirements required for safe consumption of potable water on the ISS [2].
2. Provide an approximately sized Filtration system [1].

Assumptions used for this study:

- Housing internal volume is held constant at 250 cc (15.2563 in^3) based on heritage ISS hardware to evaluate changing L/D profiles over an identical chemical payload footprint [1].
- Water density remains completely uniform and unchanging throughout the internal flow channels under low-pressure operating conditions [6].
- Low fluid velocity (500 mL/min) creates a pore Reynolds number well below 1, allowing the kinetic/turbulent term of the Ergun equation to be neglected [1, 4].
- Dynamic viscosity (μ) is maintained at a constant value of 0.00008307 lbm/(in·s), assuming a standard ambient spacecraft water bus temperature of 20°C prior to downstream thermal processing [2, 7].
- The interstitial void fraction (ϵ) remains fixed at a uniform value of 0.38 (38% void space) throughout the entire random packed bed [1, 4].
- Active resin beads are modeled as perfectly uniform, smooth, non-deformable spheres with a mean particle diameter of 0.65 mm (0.02559 in) [1].
- Calculations assume a clean "Day 1" operating condition with zero internal carbon fines shedding, particulate loading, or microbial cake formation [5, 6].

Governing Equations:

- **Ergun Equation (Viscous Component):** Used to evaluate packed bed media sizing and fluid drag dependencies [1, 4].

$$\Delta P = L \cdot \left[\frac{150 \cdot \mu \cdot V \cdot (1-\epsilon)^2}{g_c \cdot d_p^2 \cdot \epsilon^3} \right] \tag{1}$$

- **Empty Bed Contact Time (EBCT):** Used to dictate dwell parameters required for design scalability [1, 5].

$$\text{EBCT} = \frac{V_{\text{bed}}}{Q_{\text{flow}}} \tag{2}$$

- **Purificational Efficiency (E):** Used to define mass-transfer limits against incoming volatile inputs [3, 6].

$$E = \left(1 - \frac{C_{\text{effline}}}{C_{\text{influent}}}\right) \times 100 \tag{3}$$

- **Log Reduction Value (LRV):** Used to process exponential sanitation standards for safe water delivery [2, 3].

$$\text{LRV} = \log_{10}\left(\frac{C_{\text{influent}}}{C_{\text{effline}}}\right) \tag{4}$$

Variable and Parameter Reference Framework:

ΔP = Total structural bed pressure drop (psi). Core modeling structure derived from [1, 4].

L, D = Length and Diameter of the packed resin bed (in), outlined in [1].

μ = Dynamic fluid viscosity (0.00008307 lbm/(in · s)). Calculated using pure water properties at the ambient cabin temperature [2] and tabulated in [7].

V = Superficial fluid velocity (in/s), where $V = Q_{\text{flow}}/\text{Area}$. Fluid continuity transformation derived from [1, 6].

ϵ = Interstitial bed void fraction (0.38). Traced to random close packed bead constants verified in [1].

g_c = Dimensional gravitational proportionality constant (386.088 lbm · in/(lbf · s^2)), standard physical engineering conversion factor.

d_p = Mean spherical particle diameter (0.02559 in / 0.65 mm). Traced from [1].

V_{bed} = Total internal bed volume (15.2563 in^3 / 250 cc). Traced to core geometry boundaries established in [1].

Q_{flow} = Volumetric flow rate (0.50853 in^3/s / 500 mL/min). Traced to flight system supply manifolds tracked in [1].

C_{influent} = Influent contaminant concentration level (ppm or CFU/mL).

C_{effline} = Effluent contaminant concentration level ($<$ 0.2 ppm Iodine / $<$ 50 CFU/mL Microbial). Traced to baseline safety requirements in [2] and spaceflight performance data tracked in [3].

Decontamination System Computations

1. Iodine Removal Efficiency Calculation

$$E = \left(1 - \frac{0.2 \text{ ppm}}{1.0 \text{ ppm}}\right) \times 100 = 80.0\% \tag{5}$$

$$E = \left(1 - \frac{0.2 \text{ ppm}}{2.0 \text{ ppm}}\right) \times 100 = 90.0\% \tag{6}$$

2. Microbial Log Reduction Value (LRV) Calculation

$$\text{LRV} = \log_{10}\left(\frac{100,000 \text{ CFU/mL}}{50 \text{ CFU/mL}}\right) = \log_{10}(2000) \approx 3.3010 \tag{7}$$

3. Microorganism Removal Percentage Calculation

$$P(\%) = \left(1 - \frac{1}{10^{3.3010}}\right) \times 100 = \left(1 - \frac{1}{2000}\right) \times 100 = 99.95\% \tag{8}$$

Decontamination System Sizing Geometry (L/D Ratio)

$$V_{\text{target}} = \pi \cdot \left(\frac{D}{2}\right)^2 \cdot L \quad \Longrightarrow \quad L = \frac{4 \cdot V_{\text{target}}}{\pi \cdot D^2} \tag{9}$$

Table 1: Parametric Geometric Sweep for a Fixed 250 cc Filter Payload

Diameter (D, in)	Length (L, in)	Aspect Ratio (L/D)	Pressure Drop (ΔP, psi)
1.75	6.342	3.624	0.3127
2.25	3.837	1.705	0.1144
2.45	3.236	1.321	0.0814
2.75	2.569	0.934	0.0513
3.00	2.158	0.719	0.0362

MATLAB Sizing Simulation Source Code

The simulation source code provides a systematic framework for calculating, sizing, and optimizing an ideal length-to-diameter (L/D) ratio for the ACTEX resin bed based on available information in literature. The code simulates a resin bed to achieve the absolute lowest possible pressure drop to further amplify the system performance of the EBPWD. For the script to perform its primary function, a multi-variable constraint matrix evaluates the interactive trade space. The code and how it optimizes the best L/D ratio for our application is governed by the following constraints:

```
clear; clc; close all;
%% 1.) Physical System Parameters
V_target = 15.2563;        % Target volume fixed at 250 cc
Q_flow   = 0.50853;        % System volumetric flow rate
    (500 mL/min)
dp       = 0.02559;        % Resin bead diameter (0.65 mm)
mu       = 0.00008307;     % Water dynamic viscosity at 20
     C
epsilon  = 0.38;           % Packed bed void fraction
    space
gc       = 386.088;        % Gravitational unit conversion
     constant
bottom_half = gc * (dp^2) * (epsilon^3);

%% 2.) Design Constraints and Performance Targets
EBCT_design = V_target / Q_flow;

% Constraint 1: Biological Safety Target (Chick-Watson
    kinetics)
C_influent = 100000;
C_eff_max  = 50;
Target_LRV = log10(C_influent / C_eff_max);
```

```
k_media = -log(C_eff_max / C_influent) / EBCT_design;

% Constraint 2: Maximum Velocity Ceiling (Prevents bed
    compaction)
V_shear_max = 0.120;

% Constraint 3: Minimum Aspect Ratio (Prevents flow
    channeling)
LD_safety_min = 1.32;

%% 3.) Parametric Sweep Loop
D_range = 1.50 : 0.01 : 5.00;
LD_ratio = zeros(length(D_range), 1);
dP_total = zeros(length(D_range), 1);
EBCT_actual = zeros(length(D_range), 1);
LRV_achieved = zeros(length(D_range), 1);
Velocity_track = zeros(length(D_range), 1);

for i = 1:length(D_range)
    D = D_range(i);
    Area = pi * (D^2) / 4;
    L = V_target / Area;

    LD_ratio(i) = L / D;
    Velocity = Q_flow / Area;
    Velocity_track(i) = Velocity;

    % Apply a dwell time penalty if the column gets too
        shallow
    if LD_ratio(i) < 1.0
        channeling_factor = 1.0 - (1.0 - LD_ratio(i))^2;
        EBCT_actual(i) = EBCT_design * max(0.1,
            channeling_factor);
    else
        EBCT_actual(i) = EBCT_design;
    end

    % Check biological kill performance based on
        effective contact time
    C_eff_actual = C_influent * exp(-k_media *
        EBCT_actual(i));
    LRV_achieved(i) = log10(C_influent / C_eff_actual);

    % Compute the viscous pressure drop via Ergun
        equation
```

```
    top_half = 150 * mu * Velocity * ((1 - epsilon)^2);
    dP_total(i) = L * (top_half / bottom_half);
end

%% 4.) Automated Constraint Selection
% Isolate configurations that pass all 3 safety
   thresholds simultaneously
valid_indices = find(LRV_achieved >= Target_LRV & ...
                     Velocity_track <= V_shear_max & ...
                     LD_ratio >= LD_safety_min);

if isempty(valid_indices)
    error('Design␣Space␣Warning:␣No␣dimensions␣satisfy␣
       all␣safety␣margins.');
end

% Pick the safe configuration that minimizes total system
    pressure drop
[~, min_dp_idx_relative] = min(dP_total(valid_indices));
opt_idx = valid_indices(min_dp_idx_relative);

% Save optimal dimensions
D_opt   = D_range(opt_idx);
dP_opt  = dP_total(opt_idx);
LD_opt  = LD_ratio(opt_idx);
Area_opt = pi * (D_opt^2) / 4;
L_opt   = V_target / Area_opt;
EBCT_opt = EBCT_actual(opt_idx);
V_opt    = Velocity_track(opt_idx);
```

Justification of System Constraints and Optimization Trade Space

The sizing simulation is governed directly by the physical boundaries of packed bed fluid dynamics, alongside constraints derived from the design implementation and concept of the resin bed.

1. Derivation of the Lower Boundary (Media Compaction Limit)

To prevent bed compaction, the fluid's superficial velocity (V) cannot exceed 0.120 in/s [5]. Given a fixed system flow rate of $Q_{\text{flow}} = 500$ mL/min (0.50853 in^3/s) [1], the absolute minimum housing diameter (D_{min}) is derived using fluid

continuity:

$$V = \frac{Q_{\text{flow}}}{\text{Area}} \implies 0.120 \text{ in/s} = \frac{0.50853 \text{ in}^3/\text{s}}{\frac{\pi}{4} D_{\text{min}}^2} \tag{10}$$

$$D_{\text{min}}^2 = \frac{0.50853}{(0.120) \cdot \left(\frac{\pi}{4}\right)} \approx 5.3957 \text{ in}^2 \implies D_{\text{min}} = \sqrt{5.3957} \approx 2.323 \text{ in} \tag{11}$$

Dropping below 2.323 in causes high localized velocity drag forces. According to Ergun's theorems [4], this risks bead crushing and structural degradation. In turn, this degradation can induce increased pressure losses, which is highly undesirable for this flight system architecture [2].

2. Justification of the Upper Boundary (Wall Channeling Limit)

Additionally, a minimum aspect ratio limit of $L/D \geq 1.32$ was selected in consideration of the chemical residence time calculated earlier in this study.

If the column profile becomes too short and wide (low L/D), the fluid can bypass the resin bed core and stream directly down through the loose wall pathways. This phenomenon, known as wall channeling, ultimately prevents the system from reaching the required chemical residence time. Maintaining an aspect ratio of $L/D \geq 1.32$ forces stable plug-flow behavior and prevents structural fluid bypassing caused by microgravity settling or launch vibration profiles [1, 2].

3. Mathematical Optimization Conclusion

Any wider diameter drops the aspect ratio below the 1.32 boundary, causing fluid channeling failure. Thus, this specific geometry is the mathematically proven optimum for achieving the lowest possible operating pressure drop ($\Delta P = 0.0814$ psi) without risking localized system failure. It is important to note that the work provided in this section is with respect to ideal conditions. More considerations as to properly sizing this component requires more than what is viable in literature.

Below this section you will find an image of a legacy ACTEX filter used for multiple devices. Provided the derived optimal L/D ratio and the dimensions derived, it is reasonable to use the legacy ACTEX for future modeling and sizing for now.

Figure 1: Legacy ACTEX Filter used for flight-heritage system configurations.

References

[1] K. W. Larner, C. McPhail, and C. Romero, "Optimization of a Deionization Bed for an Oxygen Generator Assembly for Exploration Missions," presented at the *51st International Conference on Environmental Systems*, St. Paul, MN, USA, July 10–14, 2022, Paper ICES-2022-060.

[2] *Spaceflight Human System Standards, Volume 2: Human Factors, Space Medicine, and Environmental Health*, NASA-STD-3001, Vol. 2, Rev. B, National Aeronautics and Space Administration, Washington, DC, USA, 2022.

[3] K. P. Toon and R. W. Lovell, "International Space Station USOS Potable Water Dispenser On-Orbit Functionality Versus Design," NASA Johnson Space Center, Tech. Rep. NASA/TM—2009-214794, 2009. Available: NASA Technical Reports Server, Document ID 20090038742.

[4] S. Ergun, "Fluid flow through packed columns," *Chemical Engineering Progress*, vol. 48, no. 2, pp. 89–94, 1952.

[5] H. S. Fogler, *Elements of Chemical Reaction Engineering*, 5th ed. Boston, MA, USA: Prentice Hall, 2016.

[6] W. L. McCabe, J. C. Smith, and P. Harriott, *Unit Operations of Chemical Engineering*, 7th ed. New York, NY, USA: McGraw-Hill, 2005.

[7] F. P. Incropera, D. P. DeWitt, T. L. Bergman, and A. S. Lavine, *Fundamentals of Heat and Mass Transfer*, 6th ed. Hoboken, NJ, USA: John Wiley & Sons, 2007.

Additional computation and software:

A1 | Microbial limit (<= 50 CFU/mL)

	A	B	C	D
1	Microbial limit (<	Microbial worst c	LRV	P(%)
2	1	50	1.698970004	0.98
3	2	150	1.875061263	0.9866666667
4	3	250	1.920818754	0.988
5	4	350	1.942008053	0.9885714286
6	5	450	1.954242509	0.9888888889
7	6	550	1.962211439	0.9890909091
8	7	650	1.967815317	0.9892307692
9	8	750	1.971971276	0.9893333333
10	9	850	1.975176416	0.9894117647
11	10	950	1.977723605	0.9894736842
12	11	1050	1.979796614	0.9895238095
13	12	1150	1.981516594	0.9895652174
14	13	1250	1.982966661	0.9896
15	14	1350	1.984205733	0.9896296296
16	15	1450	1.985276743	0.9896551724
17	16	1550	1.986211716	0.9896774194
18	17	1650	1.987035023	0.9896969697
19	18	1750	1.987765544	0.9897142857
20	19	1850	1.988418127	0.9897297297
21	20	1950	1.989004616	0.9897435897
22	21	2050	1.989534566	0.9897560976
23	22	2150	1.990015779	0.9897674419
24	23	2250	1.990454682	0.9897777778
25	24	3687	2.186461896	0.9934906428
26	25	7800	2.494154594	0.9967948718
27	26	11913	2.661047794	0.9978175103
28	27	16026	2.773461374	0.9983152377
29	28	20139	2.856879871	0.9986096628
30	29	24252	2.922349562	0.9988042223
31	30	28365	2.975661533	0.9989423585
32	31	32478	3.020227584	0.9990455077
33	32	36591	3.0582243	0.999125468
34	33	40704	3.09112315	0.9991892689
35	34	44817	3.119963865	0.9992413593
36	35	48930	3.145507171	0.9992846924
37	36	53043	3.168325578	0.9993213054
38	37	57156	3.188860103	0.9993526489
39	38	61269	3.207457195	0.9993797842
40	39	65382	3.224393594	0.9994035056
41	40	69495	3.239893568	0.999424419
42	41	73608	3.254141161	0.9994429953
43	42	77721	3.267289089	0.9994596055
44	43	81834	3.279465324	0.999474546
45	44	85947	3.290778046	0.9994880566
46	45	90060	3.301319429	0.9995003331
47	46	94173	3.311168574	0.9995115373
48	47	98286	3.320393803	0.9995218037
49	48	98286	3.311250423	0.9995116293
50	49	98286	3.302295581	0.9995014549
51	50	100000	3.301029996	0.9995

Convert to table

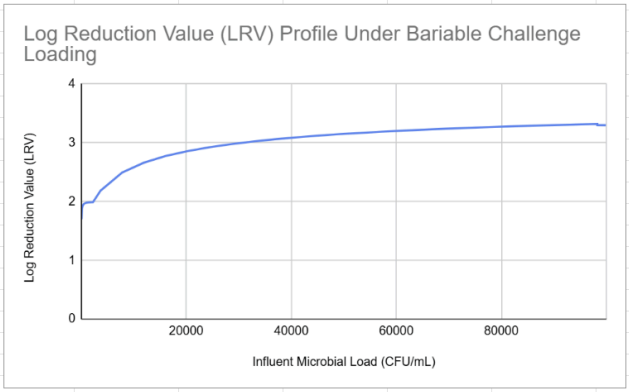

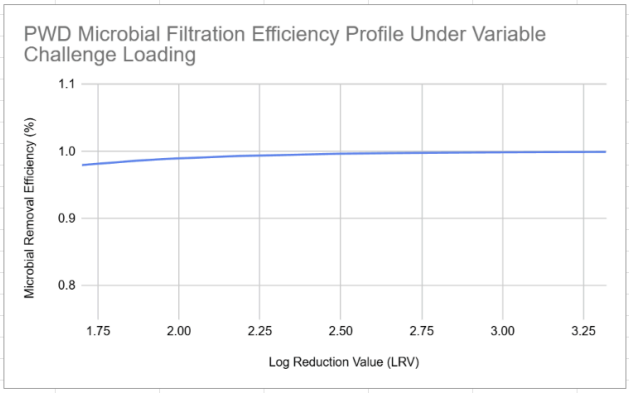

	A	B	C	D	E	F	G	H	I	J
1	Iodine concentration (ppm)	outcome (<0.2 ppm)	equation		Microbial limit (<= 50 CFU/mL)	Microbial worst case (CFU/mL)	LRV	P(%)		
2	1	0.2	0.8		1	50	1.698970004	0.98		
3	2		1		2	150	1.875061263	0.9866666667		
4	3		1		3	250	1.920818754	0.988		
5	4		1		4	350	1.942008053	0.9885714286		
6					5	450	1.954242509	0.9888888889		
7					6	550	1.962211439	0.9890909091		
8					7	650	1.967815317	0.9892307692		
9					8	750	1.971971276	0.9893333333		
10					9	850	1.975176416	0.9894117647		
11					10	950	1.977723605	0.9894736842		
12					11	1050	1.979796614	0.9895238095		
13					12	1150	1.981516594	0.9895652174		
14					13	1250	1.982966661	0.9896		
15					14	1350	1.984205733	0.9896296296		
16					15	1450	1.985276743	0.9896551724		
17					16	1550	1.986211716	0.9896774194		
18					17	1650	1.987035023	0.9896969697		
19					18	1750	1.987765544	0.9897142857		
20					19	1850	1.988418127	0.9897297297		
21					20	1950	1.989004616	0.9897435897		
22					21	2050	1.989534566	0.9897560976		
23					22	2150	1.990015779	0.9897674419		
24					23	2250	1.990454682	0.9897777778		
25					24	3687	2.186461896	0.9934906428		
26					25	7800	2.494154594	0.9967948718		
27					26	11913	2.661047794	0.9978175103		
28					27	16026	2.773461374	0.9983152377		
29					28	20139	2.856879871	0.9986096628		
30					29	24252	2.922349562	0.9988042223		
31					30	28365	2.975661533	0.9989423585		
32					31	32478	3.020227584	0.9990455077		
33					32	36591	3.0582243	0.999125468		
34					33	40704	3.09112315	0.9991892689		
35					34	44817	3.119963865	0.9992413593		
36					35	48930	3.145507171	0.9992846924		
37					36	53043	3.168325578	0.9993213054		
38					37	57156	3.188860103	0.9993526489		
39					38	61269	3.207457195	0.9993797842		
40					39	65382	3.224393594	0.9994035056		
41					40	69495	3.239893568	0.999424419		
42					41	73608	3.254141161	0.9994429953		
43					42	77721	3.267289089	0.9994596055		
44					43	81834	3.279465324	0.999474546		
45					44	85947	3.290778046	0.9994880566		
46					45	90060	3.301319429	0.9995003331		
47					46	94173	3.311168574	0.9995115373		
48					47	98286	3.320393803	0.9995218037		
49					48	98286	3.311250423	0.9995116293		
50					49	98286	3.302295581	0.9995014549		
51					50	100000	3.301029996	0.9995		
52										
53										
54										
55										
56										

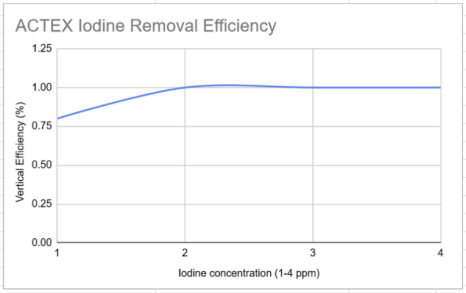

Disclaimer: all computation and units were done with respect to inches and english units

Preliminary Budget

Table 1: Preliminary Budget for Dispenser Ground Unit. *denotes estimate

Category	Line-Item	Description	Amount ($)
Income	Grant Funding	CaSGC Grant	$2,500.00
	NASA Funding	HuLC Phase 2	$9,000.00
			$11,500.00
Expenses	**Non-Personnel Costs**		

	*Bill of Materials	Cost of Development	$4,504.04
	Travel: Flights, Hotel, Ground Transportation	Transportation to HuLC Forum for 3 Team Members	$5,351.00
	Contingency Reserve	Reserve for unforeseen or unexpected expenses	$1,644.96

System Requirements

Table 2: System Level Requirements

Req. ID	Req.	Rationale	Parent Req.	Child Req.	Verification Method	Req. Met?
MG-1	Enhance life support functionality through safer water delivery while considering the integrated nature of ECLSS within future exploration architectures.	Mission Goal	-	All	Analysis	Met
PM-1	The system shall have targeted use within 5 to 8 years, or be ready between March 1, 2031 and March 1, 2034.	Customer Constraint (Schedule)	MG-1	-	Analysis	Met
PM-2	The system shall be designed for a crew of 4 for cislunar, lunar, and/or Martian environments as applicable.	Customer Constraint	SLS-SPEC-159	MR-5.2, MR-4	Analysis	Met
PM-3	The system shall be designed for deployment on or implementation within NASA/commercial HLS lunar surface or Mars transit assets.	Customer Constraint	MG-1	MR-1, MR-3	Analysis	Met

PM-4	The budget for the system development shall not exceed $11500 USD.	System Constraint (Budget)	MG-1	-	Analysis	Met
MR-1	The system shall have minimal barriers to NASA adoption (e.g., low mass, small size, low power, etc.).	Customer Constraint	MG-1	MR-1.1, MR-1.2, MR-1.3	Analysis	Met
MR-1.1	The system shall not exceed a total mass of 15 kg.	System Constraint	MR-1	-	Analysis, Inspection	In Progress
MR-1.2	The system shall not exceed 0.47 m x 0.28 m x 0.55 m in stowed configuration.	Size of Space Shuttle Middeck Lockers and previous potable water dispensers designs.	MR-1	-	Analysis, Inspection	In Progress
MR-1.3	During operation, the system shall receive no more than 28 Vdc of power.	Power draw from EXPRESS Rack 6 of current ISS Potable Water Dispenser	MR-1	-	Analysis, Test	In Progress
MR-2	The system shall add no additional risks posed to crew.	Customer Constraint	MG-1	MR-2.1	Analysis	Met
MR-2.1	The system's microbial water quality limit shall be less than or equal to 50 CFU/mL for potable water.[7,8]	System Constraint	MR-2	-	Test	Not Met
MR-3	The system shall have the ability to survive launch loads.	Customer Constraint	MG-1	-	Analysis, Test	In Progress
MR-4	The system must have a mission	Customer Constraint	MG-1	-	Analysis	Met

	operational life of 30-days for lunar surface missions, or 1200-days for Mars missions					
MR-5	The system shall be able to safely and efficiently deliver temperature-controlled water for astronauts' food and beverage needs, emphasizing ergonomics and throughput while minimizing waste and cleaning requirements.	Customer Constraint	MG-1	MR-5.1, MR-5.2	Test	Not Met
MR-5.1	Water shall be dispensed at 25 mL increments.[7,8]	On the ISS, water is dispensed in fixed increments to properly hydrate food and beverages without overflow, while aligning with preparation instructions and meal schedule constraints.	MR-5, NASA-STD-3001	-	Test	Not Met
MR-5.2	For hydration, the dispenser shall provide a minimum of 2.5 L (84.5 fl oz) per crewmember per day.[7,8]	System Constraint	MR-5, NASA-STD-3001	-	Test	Not Met
MR-6	The system shall be able to withstand environmental effects such as corrosion.	System Constraint	MG-1	-	Inspection	Not Met

Subsystem Requirements

Table 3: Thermal Subsystem Requirements

Req. ID	Req.	Rationale	Parent Req.	Child Req.	Verification Method	Req. Met?
TH-1	The heater shall provide hot water at a temperature range between 68°C (155°F) and 79°C (175°F).	Subsystem Constraint	MR-5.2, NASA-STD-3001	-	Analysis, Test	In Progress
TH-2	The evaporator shall provide cold water at a temperature of at least 16°C (60°F).	Subsystem Constraint	MR-5.2, NASA-STD-3001	-	Analysis, Test	In Progress
TH-3	The evaporator and heater shall be capable of producing nominal/ambient water at a temperature between 18°C (64°F) and 27°C (81°F).	Subsystem Constraint	MR-5.2, NASA-STD-3001	-	Analysis, Test	In Progress
TH-4	The system shall be capable of monitoring and responding to temperature of the water at critical points throughout the pipe circuit.	Critical points that need temperature measurements are evaporator and heater inlets/outlets.	MR-5	-	Analysis, Test	In Progress

Table 4: Electrical Subsystem Requirements

Req. ID	Req.	Rationale	Parent Req.	Child Req.	Verification Method	Req. Met?
EE-1	The system shall receive power from ISS EXPRESS Rack 6.	Subsystem Constraint	MR-1.3	-	Analysis	Met

Table 5: Structural Subsystem Requirements

Req. ID	Req.	Rationale	Parent Req.	Child Req.	Verification Method	Req. Met?
SC-1	The system will incorporate check valves to prevent backflow and ensure one-way transport of water.	Previous potable water systems incorporated check valves to prevent backflow and potential leakage.	MR-2	-	Analysis	Met
SC-2	The system shall be capable of monitoring and responding to the pressure of the water at critical points throughout the pipe circuit.	Critical points that need pressure measurements are the inlets/outlets of the heater and evaporator, as well as the dispenser inlet.	MR-5	-	Analysis	Met
SC-3	The system will incorporate a temperature switch to ensure the designated water temperature is met.	Previous PWD iterations have utilized temperature switches to dispense potable water at desired temperatures.	MR-5	-	Analysis	Met
SC-4	System components that require replacement will have quick disconnects (QD) for easy maintenance and access.	Allows for easy access, replacements, and maintenance for vital components.	MR-5	-	Analysis	Met
SC-5	The system shall minimize pressure	Previous PWD iterations had	MR-5	-	Analysis, Test	In Progr

	losses to prevent reductions in potable water flow rate and to ensure accurate dispensing.	complications with pressure dropping. Resulted in inaccurate dispense volumes.				ess

Table 6: Decontamination Subsystem Requirements

Req. ID	Req.	Rationale	Parent Req.	Child Req.	Verification Method	Req. Met?
DC-1	The system shall include deiodination and microbial filters to ensure the water quality limit is less than or equal to 50 CFU/mL.	Subsystem Constraint	MR-2.1, MR-5	-	Analysis, Test	In Progress
DC-2	The system shall be capable of replacing the filters.	Subsystem Constraint	MR-5	-	Analysis	Met

Gantt Chart

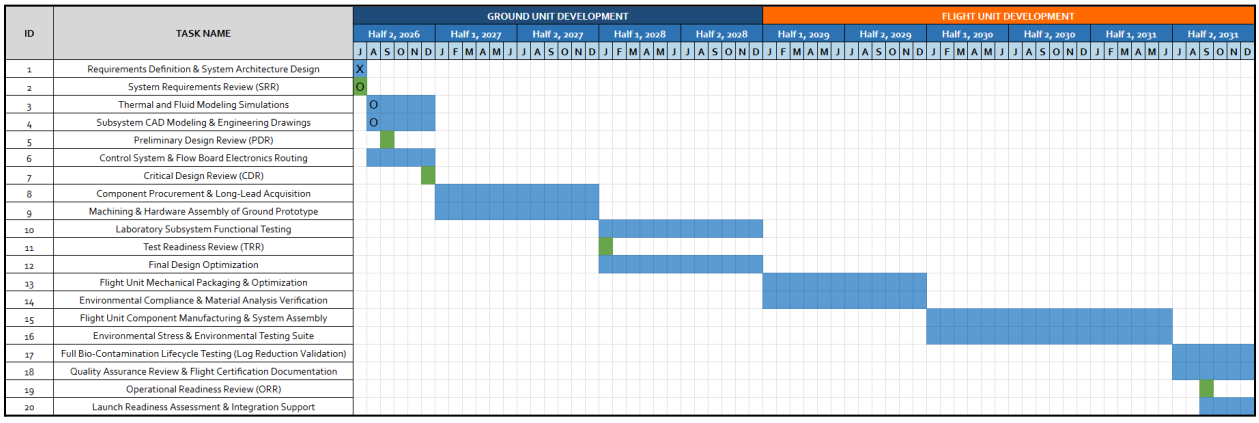

Note: X denotes completed task and O denotes in-progress task.

P&ID Key

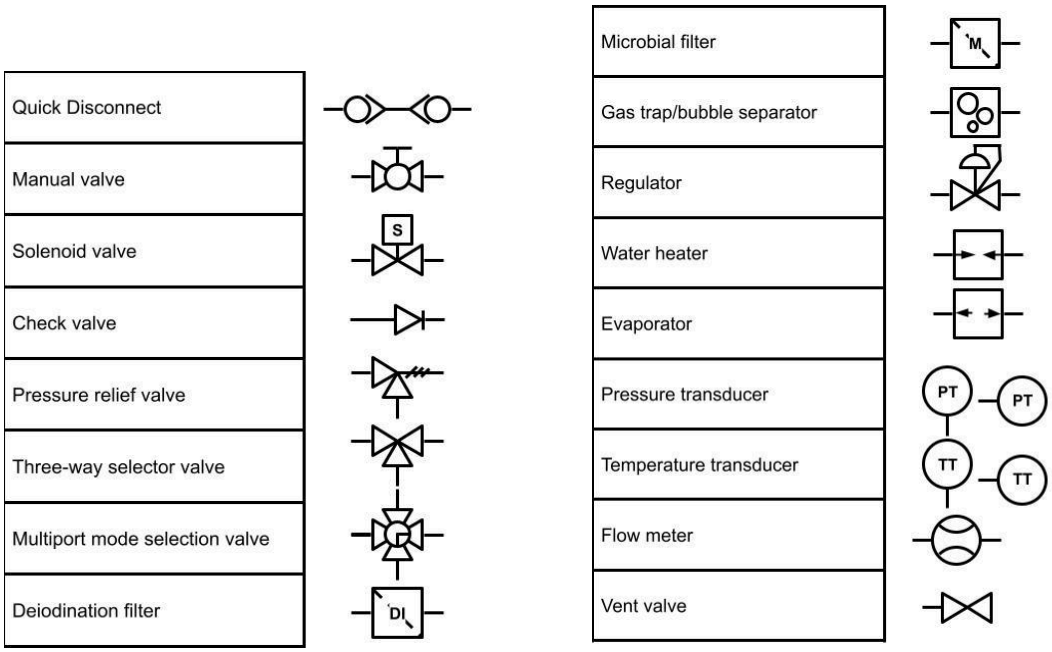
Quick Disconnect
Manual valve
Solenoid valve
S
Check valve
Pressure relief valve
Three-way selector valve
Multiport mode selection valve
Deiodination filter
DI
Microbial filter
M
Gas trap/bubble separator
Regulator
Water heater
Evaporator
Pressure transducer
PT
PT
Temperature transducer
TT
TT
Flow meter
Vent valve